

We are IntechOpen, the world's leading publisher of Open Access books Built by scientists, for scientists

6,900

Open access books available

186,000

International authors and editors

200M

Downloads

Our authors are among the

154

Countries delivered to

TOP 1%

most cited scientists

12.2%

Contributors from top 500 universities



WEB OF SCIENCE™

Selection of our books indexed in the Book Citation Index
in Web of Science™ Core Collection (BKCI)

Interested in publishing with us?
Contact book.department@intechopen.com

Numbers displayed above are based on latest data collected.
For more information visit www.intechopen.com



Heat Transfer Enhancement Technique of PCMs and Its Lattice Boltzmann Modeling

Zhiguo Qu

Abstract

Phase change materials (PCMs) have several advantages for thermal energy storage due to their high energy storage density and nearly constant working temperature. Unfortunately, the low thermal conductivity of PCM impedes its efficiency of charging and discharging processes. To solve this issue, different techniques are developed to enhance the heat transfer capability of PCMs. In this chapter, the common approaches, which include the use of extended internal fins, porous matrices or metal foams, high thermal conductivity nanoparticles, and heat pipes for enhancing the heat transfer rate of PCMs, are presented in details. In addition, mathematical modeling plays a significant role in clarifying the PCM melting and solidification mechanisms and directs the experiments. As a powerful mesoscopic numerical approach, the enthalpy-based lattice Boltzmann method (LBM), which is robust to investigate the solid-liquid phase change phenomenon without iteration of source terms, is also introduced in this chapter, and its applications in latent heat thermal energy storage (LHTES) unit using different heat transfer enhancement techniques are discussed.

Keywords: phase change materials, heat transfer enhancement, nanofluid, mathematical models, lattice Boltzmann method

1. Introduction to heat transfer enhancement techniques of PCMs

The development of renewable energy such as solar energy and wind energy has attracted lots of attention during the past decades due to the gap between the increased global energy demand and the decreased amount of fossil fuel in the world. However, one of the major drawbacks for renewable energy is its territorial, time-dependent, and intermittent characteristics. Under this circumstance, the energy storage techniques play an indispensable role for achieving a continuous and reliable supply of renewable energy [1, 2]. Thermal energy storage (TES), which stores the heat in the materials and generates the electricity with heat engine cycles later, is a promising energy storage technique. In general, TES could be classified into three different categories, namely latent, sensible, and thermochemical. With the advantages of high energy storage density and nearly constant charging/discharging temperature, latent heat thermal energy storage (LHTES) using phase change materials (PCMs) is widely used in several renewable energy applications. However, a major issue of LHTES system is the low thermal conductivity of most

PCMs, which seriously impedes the energy storage efficiency. To handle this challenge, several heat transfer enhancement techniques are developed and discussed by researches during the past years. The existing effective approaches to ameliorate the thermal performance of PCMs include using extended internal fins, filling porous matrix or metal foams, adding high thermal conductivity nanoparticles, and using heat pipes [3].

With the characteristics of simple fabrication, low cost construction, and large heat transfer surfaces, fins are used in a majority of PCM-based LHTES systems. There are several different configurations of fins such as longitudinal, annular, circular, plates, pins, tree shape, and other novel geometries as shown in **Figure 1** [4]. By applying extended internal fins, the average thermal conductivity and heat transfer depth of LHTES system are improved, so that the melting and solidification rate of PCMs are accelerated. However, there exists a tradeoff between the increased PCM charging/discharging rate in LHTES unit and its corresponding reduced energy storage capacity with the existence of internal fins. An optimum design of fin configuration and arrangement becomes significant for achieving high energy storage efficiency of LHTES unit with PCMs. Under this circumstance, lots of researches are numerically and experimentally carried out to investigate the conjugate heat transfer between fins and PCMs, and the enhancement of PCM thermal performance with different type of fins is deeply understood and optimized during the recent years [5–21].

Due to the high surface area to volume ratio generated by the tortuosity of metal foams as shown in **Figure 2**, the PCM charging/discharging rates could be highly improved by inserting metal foams into the LHTES unit [22]. As air inevitably exists

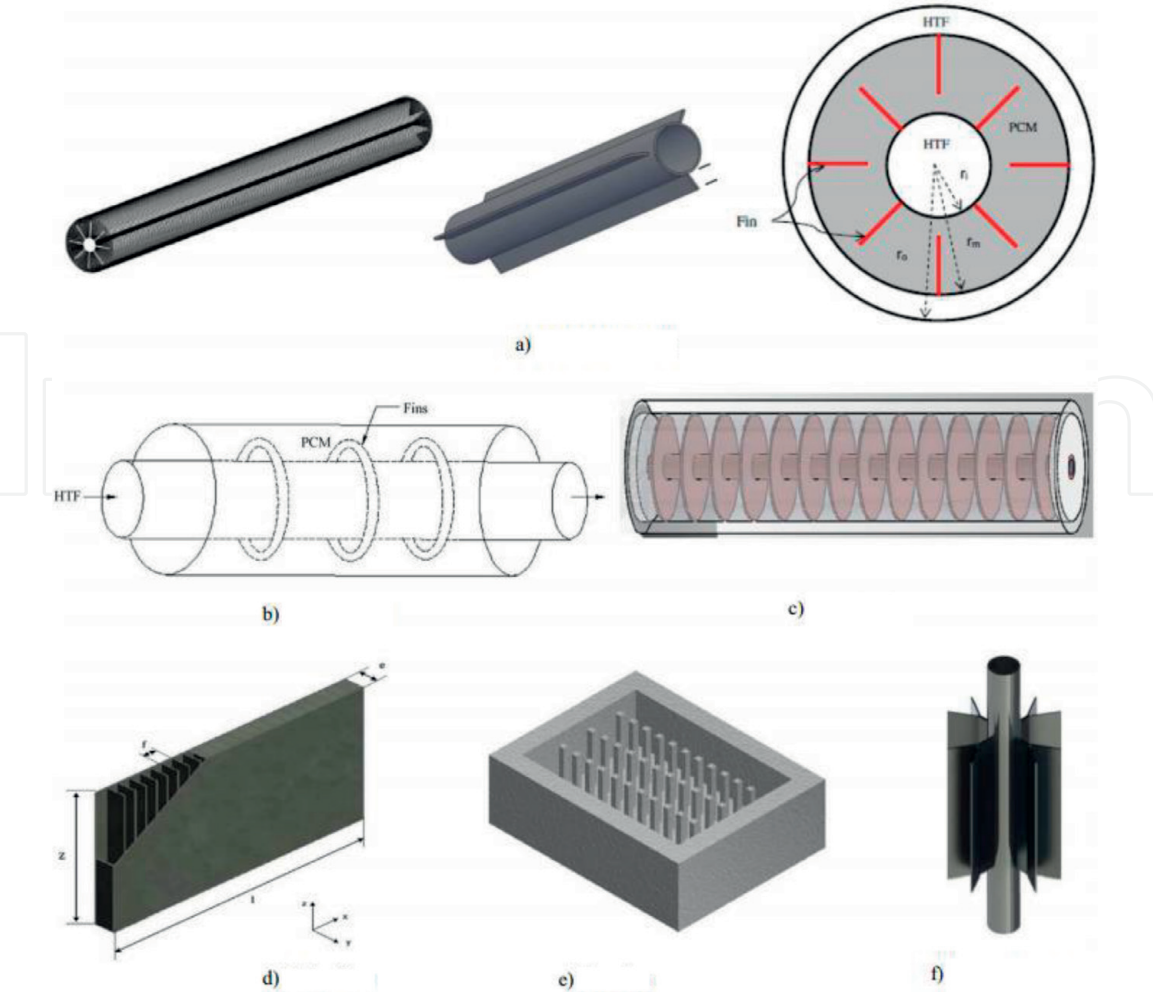


Figure 1.
Different configuration of fins used in LHTES system with PCMs [4].

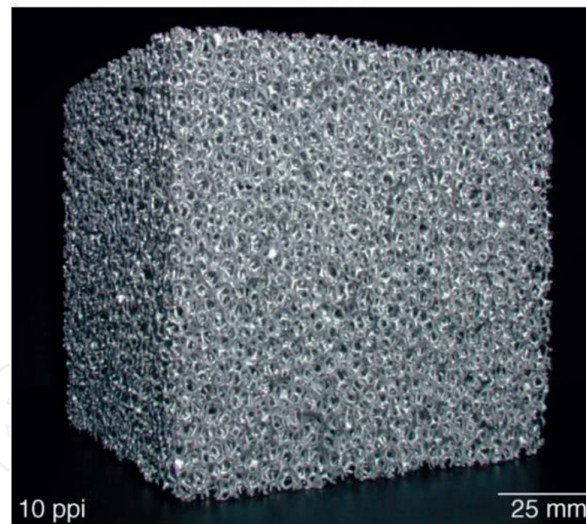


Figure 2.
 A piece of FeCrAlY foam sample manufactured with the sintering route [22].

in the porous structure of metal foams, the infiltration of PCMs into metal foams is hindered, which correspondingly reduces the impregnation ratio of PCMs. As a consequence, the energy storage capacity of LHTES system using combination of PCMs and metal foams is affected. To handle this difficulty, a vacuum impregnation method is generally used to prepare the PCM/metal foam composite materials. **Figure 3** shows the apparatus and procedures of impregnation treatment for PCMs with vacuum assistance, and the detailed steps could be found in Ref. [23]. As the PCM melting and solidification are actually accelerated due to the interconnected heat transfer channel inside the metal foams, the porosity and pore size of metal foams are the most significant factors, which affect the energy storage efficiency of LHTES. The copper foam with different porosities and pore sizes is displayed in **Figure 4** as an example [24]. The conduction heat transfer in the LHTES system could be consolidated with the decrement of porosity and pore sizes because of the increased density of high speed heat transfer channels inside the metal foams. However, natural convective heat transfer of liquid PCMs through the metal foams is hampered due to the reduced void space caused by the decreased metal foam porosity and pore size. In addition, when the porosity of metal foams decreases, the amount of pure PCMs in the LHTES unit is reduced, which decreases the energy storage capacity. Due to the above reasons, metal foams with appropriate porosity, pore size, and filling ratio, which balance the conduction and natural convection, are essential for achieving the optimum heat transfer rate of PCMs and the most efficient energy storage of LHTES unit. Hence, the mechanisms of PCM melting and solidification processes inserted with various metal foams are studied by several researches at both macroscopic and pore scales [25–44]. Besides, the heat transfer rate of PCMs could also be ameliorated by applying other additives such as graphite [45, 46], carbon nanotubes [47], and graphene [48].

As the nanotechnology has achieved rapid development during the past decades, adding high thermal conductivity nanoparticles becomes a new technique to improve the low heat transfer rate of PCMs [49]. Khodadadi and Hosseinzadeh first investigated the enhancement of PCM heat transfer capability using nanoparticles [50], and their results demonstrated that nanoparticle-enhanced PCMs (NEPCMs) have a great potential in TES applications. The SEM micrographs of nanoparticle-enhanced PCM ($\text{NaNO}_3\text{-KNO}_3$) with different nanoparticles and mass fractions are shown in **Figure 5** [51]. With the existence of nanoparticles, the thermophysical properties of PCMs such as thermal conductivity and latent heat capacity are varied. The mechanism of the effects of surface, chemical, and physical

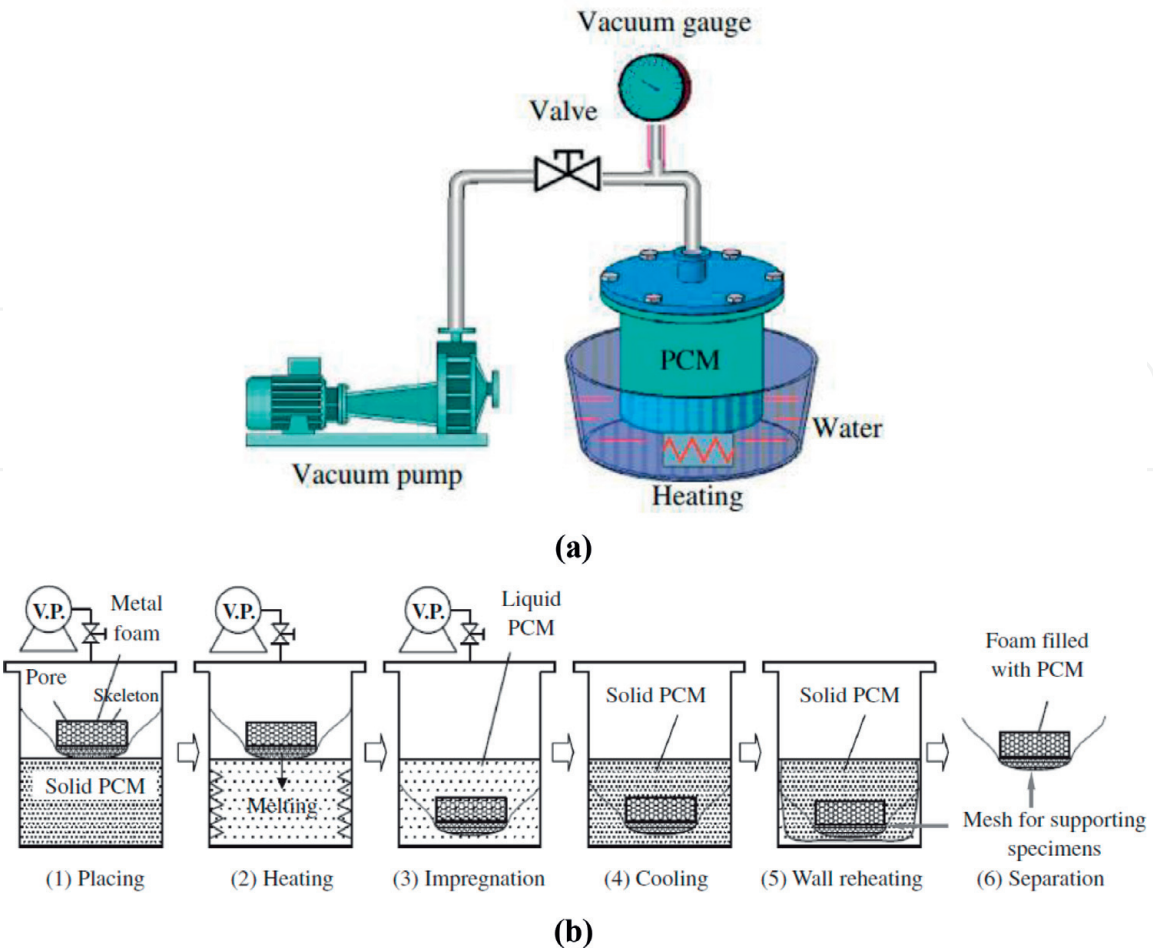


Figure 3. Schematic of the apparatus and procedure for the preparation of composite PCMs using a vacuum impregnation method [23].

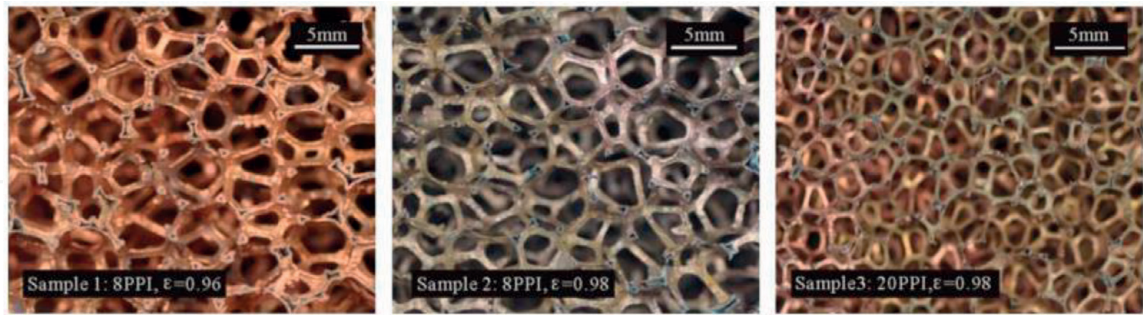


Figure 4. Copper foam samples with different pore sizes and porosities [24].

properties of nanoparticles on the thermal properties of PCMs is reviewed in Ref. [52]. In the recent years, many researches related to NEPCMs are carried out, which mainly focus on enhancing the charging/discharging speed of PCMs with nanoparticles [53–73]. However, although the effective thermal conductivity of PCMs is ameliorated by adding nanoparticles, the energy storage capacity of LHTES unit is decreased. Furthermore, the use of nanoparticles increases the viscosity of PCMs, which impedes the development of natural convective heat transfer. Under this circumstance, the total heat transfer rate of PCMs may decrease especially for the cases under high temperature with dominant convective heat transfer. Compared with melting/solidification rate of PCMs, the energy storage rate of LHTES system is the essential goal of storing heat using PCMs. Hence, more investigations, which concentrate on the energy storage rate of NEPCM, should be completed in

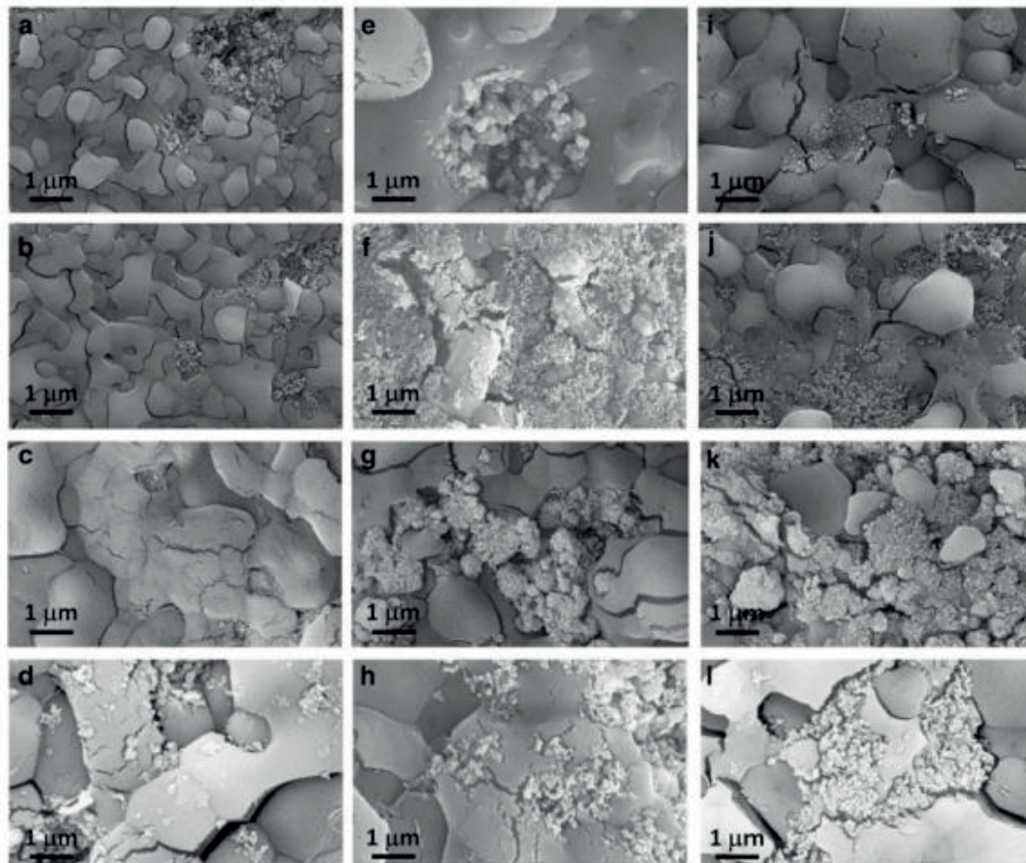
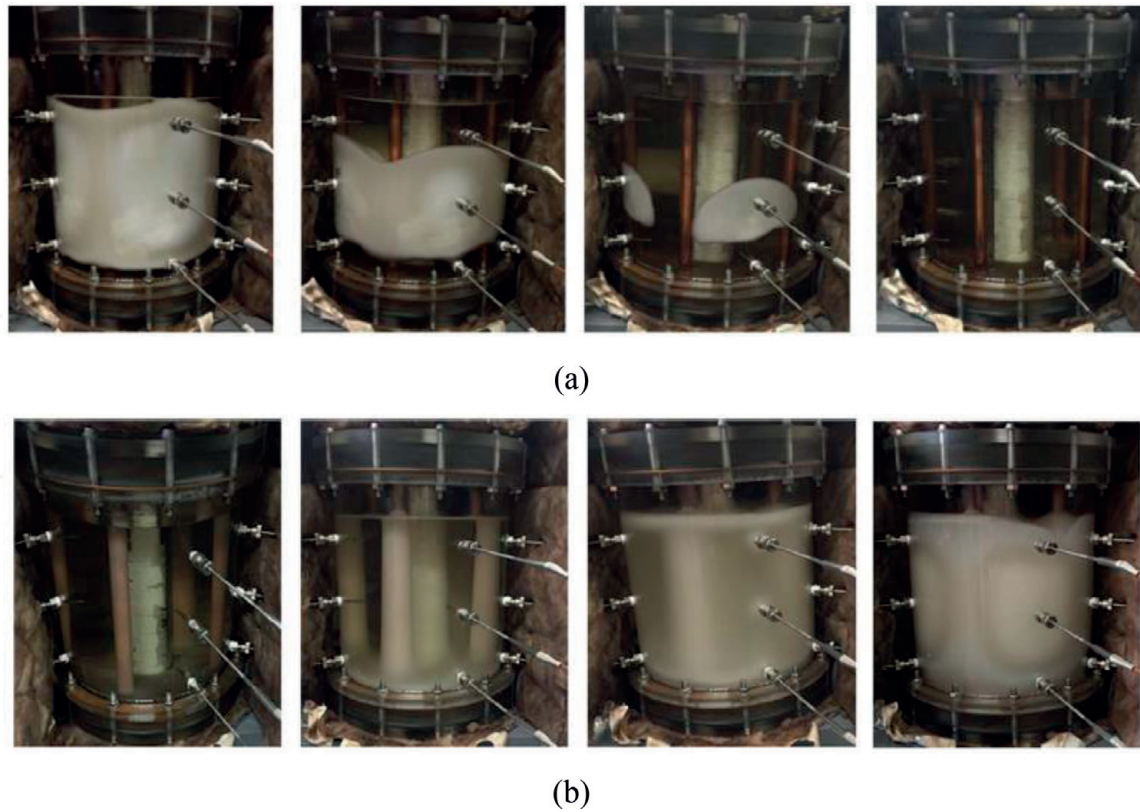


Figure 5.
 SEM photos of nanoparticle-enhanced $\text{NaNO}_3\text{-KNO}_3$ with 0.5 wt.% (a–d), 1.0 wt.% (e–h), and 1.5 wt.% (i–l) of nanoparticles. Silica (a, e, i), alumina (b, f, j), titania (c, g, k), and alumina-silica nanoparticles (d, h, l) [51].

the future research, and the technique of adding nanoparticles for enhancing the thermal performance of LHTES needs to be further compared with other heat transfer improvement technologies in order to realize the optimum energy storage efficiency.

As the most commonly used heat exchanger devices, heat pipes are widely used to amplify the charging/discharging processes of PCMs and to transfer heat from a source to the storage or from the storage to a sink with heat transfer fluid (HTF) [74]. Although increasing the heat transfer area on the PCM side using extended fins or metal foams is the most efficient and simple method to ameliorate the energy storage rate of LHTES system as previously discussed, when there exists high temperature HTF passing through the LHTES tank such as the waste heat recovery, heat pipes are indispensable for achieving the high efficiency energy storage. The transient charging/discharging processes of PCMs in a LHTES unit with heat pipes are shown in **Figure 6** [75]. The configuration and arrangement of heat pipes play a significant role in the energy storage rate of PCMs. To optimize the thermal performance of heat pipe-assisted LHTES systems, lots of experimental and numerical works are carried out during the past few years [76–96].

The significant research progress of PCM heat transfer enhancement using a single technique is discussed and summarized in the above paragraphs. Recently, to further improve the heat transfer capability of PCM and compare the effectiveness of different approaches (use of fins, metal foams, nanoparticles, or heat pipes), the charging/discharging processes of PCMs with hybrid heat transfer enhancement techniques are investigated. Although adding nanoparticles could ameliorate the effective thermal conductivity of PCMs, the heat transfer area on the PCM side is not improved. Based on this, the extended fins are considered to be used for

**Figure 6.**

The transient charging/discharging processes of PCM in a LHTES tank with HTF passing through heat pipes [75]. (a) Charging process and (b) discharging process.

enhancing the heat transfer depth of NEPCM in a LHTES unit [97–100]. Darzi et al. studied the melting and solidification of PCM enhanced with radial fins and nanoparticles in cylindrical annulus, and they found that adding fins on the hot or cold tubes is the best approach to expedite the heat transfer rate [98]. Lohrasbi et al. optimized the copper nanoparticle-PCM solidification process in a fin-assisted LHTES system [99]. The results indicate that immersing fin in LHTES unit increases the solidification rate more significantly than dispersing nanoparticles. Parsazadeh and Duan investigated the effects of fins and nanoparticle in a shell and tube LHTES unit [100]. They found that adding Al_2O_3 nanoparticles even decreases the overall heat transfer rate because the thermal conductivity enhancement with nanoparticles could not compensate for the natural convection reduction. Similarly, porous matrices are also inserted into the LHTES unit to improve the thermal performance of NEPCM [101, 102]. Hossain et al. studied the melting process of NEPCM inside the porous medium [101], and it is observed that the movement of PCM melting front is more significant under the influence of porous medium than that of nanoparticles. Tasnim et al. investigated the convection effect on the melting process of NEPCM filled in porous enclosure [102]. The results showed that both the conduction and convection heat transfer are degraded by the presence of nanoparticles. From these researches, it could be found that using extended fins or porous matrices is more effective than adding nanoparticles for enhancing the charging/discharging rate of LHTES system. Besides, other hybrid heat transfer enhancement techniques for enhancing the energy storage rate of LHTES with PCMs such as combination of fins and metal foams [103] or using combined three techniques [104–107] are also recently studied and analyzed.

In this chapter, the mathematical models for PCM charging and discharging processes with different heat transfer enhancement techniques are shown. In addition, the lattice Boltzmann method (LBM) for solid-liquid phase change

phenomenon is reviewed with some classical analytical and numerical validation cases, and the implementation of graphic processor unit (GPU) computing is also presented. Furthermore, the applications of LBM modeling for LHTES system with various heat transfer improvement approaches are discussed.

2. Mathematical models

2.1 Governing equations of fluid flow and solid-liquid phase change

To simulate the charging and discharging processes of PCMs, the following assumptions are usually made to simplify the mathematical models: (1) the fluid flow of liquid PCMs is Newtonian, laminar, and incompressible with negligible viscous dissipation and (2) the thermophysical properties of PCMs, nanoparticles, fins, and metal foams are constant, except the PCM density ρ , which is a linear function of temperature T using the Boussinesq approximation. Based on the above assumptions, the flow of liquid PCMs is governed by the continuity equation and the momentum equation expressed in the Cartesian coordinate as:

$$\frac{\partial u}{\partial x} + \frac{\partial v}{\partial y} + \frac{\partial w}{\partial z} = 0 \quad (1)$$

$$\rho \left(\frac{\partial u}{\partial t} + u \frac{\partial u}{\partial x} + v \frac{\partial u}{\partial y} + w \frac{\partial u}{\partial z} \right) = -\frac{\partial p}{\partial x} + \mu \left(\frac{\partial^2 u}{\partial x^2} + \frac{\partial^2 u}{\partial y^2} + \frac{\partial^2 u}{\partial z^2} \right) \quad (2)$$

$$\rho \left(\frac{\partial v}{\partial t} + u \frac{\partial v}{\partial x} + v \frac{\partial v}{\partial y} + w \frac{\partial v}{\partial z} \right) = -\frac{\partial p}{\partial y} + \mu \left(\frac{\partial^2 v}{\partial x^2} + \frac{\partial^2 v}{\partial y^2} + \frac{\partial^2 v}{\partial z^2} \right) + (\rho\beta)g(T - T_r) \quad (3)$$

$$\rho \left(\frac{\partial w}{\partial t} + u \frac{\partial w}{\partial x} + v \frac{\partial w}{\partial y} + w \frac{\partial w}{\partial z} \right) = -\frac{\partial p}{\partial z} + \mu \left(\frac{\partial^2 w}{\partial x^2} + \frac{\partial^2 w}{\partial y^2} + \frac{\partial^2 w}{\partial z^2} \right) \quad (4)$$

where ρ is the density; p is the pressure; μ is the dynamic viscosity; t is the time; β is the thermal expansion coefficient of PCMs; g is the magnitude of gravitational acceleration; T is the temperature; T_r is the reference temperature; x is the horizontal coordinate; y is the vertical coordinate; z is the coordinate, which is orthogonal with x and y coordinates; and u , v , and w are the fluid velocities in the x , y , and z directions, respectively.

The solid-liquid phase change process of PCMs is governed by the enthalpy equation as:

$$\frac{\partial(\rho H)}{\partial t} + \rho c_p \left(u \frac{\partial T}{\partial x} + v \frac{\partial T}{\partial y} + w \frac{\partial T}{\partial z} \right) = k \left(\frac{\partial^2 T}{\partial x^2} + \frac{\partial^2 T}{\partial y^2} + \frac{\partial^2 T}{\partial z^2} \right) \quad (5)$$

where c_p and k are the specific heat and thermal conductivity of PCMs. The enthalpy H of PCMs is defined as:

$$H = c_p(T - T_r) + f_l L \quad (6)$$

where f_l is the PCM liquid fraction, and L is the latent heat of PCMs. By calculating the enthalpy H of PCMs, the liquid fraction f_l and temperature T could be updated by the following equations:

$$f_l = \begin{cases} 0, & H \leq H_s \\ \frac{H - H_s}{H_l - H_s}, & H_s < H < H_l \\ 1 & H \geq H_l \end{cases} \quad (7)$$

$$T = \begin{cases} T_m - \frac{H_s - H}{c_p}, & H \leq H_s \\ T_m, & H_s < H < H_l \\ T_m + \frac{H - H_l}{c_p} & H \geq H_l \end{cases} \quad (8)$$

where H_s is the enthalpy of solid state PCMs, H_l is the enthalpy of liquid state PCMs, and T_m is the melting/solidification temperature of PCMs.

2.2 Nanofluid models

For simulating the fluid flow and heat transfer of nanoparticle-enhanced PCMs (NEPCMs), the nanoparticle is assumed to be spherical in shape, so that the Brinkman model and the Maxwell model for nanofluid are valid. In addition, the NEPCMs are considered as continuous media with the thermal dispersion being neglected. Based on this, the effective viscosity of NEPCMs is computed using the Brinkman model as [108]:

$$\mu_{nf} = \frac{\mu_{PCM}}{(1 - \Phi)^{2.5}} \quad (9)$$

where Φ is the volume fraction of nanoparticles, μ_{PCM} is the dynamic viscosity of pure PCM, and μ_{nf} is the dynamic viscosity of NEPCMs. The thermal conductivity of NEPCMs is calculated according to the Maxwell model as [109]:

$$\frac{k_{nf}}{k_{PCM}} = \frac{k_p + 2k_{PCM} - 2(k_{PCM} - k_p)\Phi}{k_p + 2k_{PCM} + (k_{PCM} - k_p)\Phi} \quad (10)$$

where k_{PCM} , k_p , and k_{nf} are the thermal conductivities of pure PCMs, nanoparticles, and NEPCMs, respectively. Furthermore, the density of nanofluid ρ_{nf} is computed using interpolation as:

$$\rho_{nf} = (1 - \Phi)\rho_{PCM} + \Phi\rho_p \quad (11)$$

where ρ_{PCM} and ρ_p are the densities of pure PCM and nanoparticles. The heat capacitance of NEPCMs $(\rho c_p)_{nf}$ is defined as:

$$(\rho c_p)_{nf} = (1 - \Phi)(\rho c_p)_{PCM} + \Phi(\rho c_p)_p \quad (12)$$

where $(\rho c_p)_{PCM}$ is the heat capacitance of pure PCM, and $(\rho c_p)_p$ is the heat capacitance of nanoparticles. The thermal expansion volume of NEPCMs $(\rho\beta)_{nf}$ is given as:

$$(\rho\beta)_{nf} = (1 - \Phi)(\rho\beta)_{PCM} + \Phi(\rho\beta)_p \quad (13)$$

where $(\rho\beta)_{PCM}$ and $(\rho\beta)_p$ are the thermal expansion volume of pure PCM and nanoparticles, respectively. The latent heat of NEPCMs $(\rho L)_{nf}$ is computed as:

$$(\rho L)_{nf} = (1 - \Phi)(\rho L)_{PCM} \quad (14)$$

where $(\rho L)_{PCM}$ is the latent heat of pure PCM. Then, the corresponding enthalpy of NEPCMs H_{nf} is given as:

$$H_{nf} = c_{p,nf}(T - T_r) + f_l L_{nf} \quad (15)$$

2.3 Conjugate heat transfer between PCMs and fins or metal foams

When the extended fins or metal foams are used as the heat transfer enhancement techniques for LHTES unit, the conjugate heat transfer occurs between the PCMs and the fins or metal foams. The heat transfer inside the fins or metal foams is governed by the conduction equation as:

$$\rho_s c_{p,s} \frac{\partial T}{\partial t} = k_s \left(\frac{\partial^2 T}{\partial x^2} + \frac{\partial^2 T}{\partial y^2} + \frac{\partial^2 T}{\partial z^2} \right) \quad (16)$$

ρ_s , $c_{p,s}$, and k_s are the density, specific heat, and thermal conductivity of fins or metal foams, respectively. On the interface of PCMs and fins or metal foams, the coupled Dirichlet-Neumann boundary conditions for conjugate heat transfer should be satisfied:

$$-k_{PCM} \frac{\partial T_{PCM}}{\partial n} = -k_s \frac{\partial T_s}{\partial n} \quad (17)$$

$$T_{PCM} = T_s \quad (18)$$

T_{PCM} and T_s are the temperature of PCMs and fins or metal foams, k_{PCM} is the thermal conductivity of PCMs, and n is the normal unit of the interface. The above boundary conditions could be satisfied in the lattice Boltzmann method automatically by using the harmonic mean value of thermophysical properties of PCMs and fins or metal foams as discussed in the following section. To investigate the melting and solidification processes of PCMs filled with metal foams at pore scale, the morphology of the real metal foam structures could be reconstructed using the

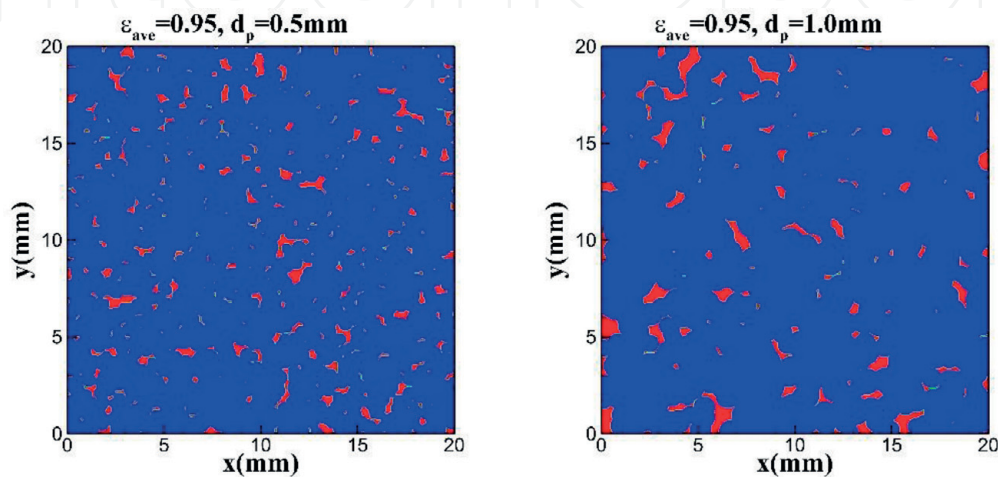


Figure 7.
 Reconstructed PCM filled with metal foams using QSGS [111].

quartet structure generation set (QSGS) as shown in **Figure 7** [110, 111], where ε_{ave} and d_p are the porosity and the pore size of metal foams. Besides, the metal foams could also be reconstructed with scanning electron microscopy (SEM).

3. Lattice Boltzmann method for solid-liquid phase change

3.1 The development history of enthalpy-based LBM for solid-liquid phase change

As a mesoscopic numerical approach developed during the past more than two decades, the lattice Boltzmann method (LBM) has become a powerful tool for simulating complex heat transfer and fluid flow problems such as single-phase flows, multiphase flows, turbulence flows, flows in porous media, heat transfer, phase change, and transport in microfluidics [112–115]. The mesoscopic nature of LBM makes it appropriate for tackling the evolvement of solid-liquid interface during the phase change process. The existing LBM for solid-liquid phase change problems could be generally categorized as follows: (1) the phase-field based method, (2) the enthalpy-based method, and (3) the immersed boundary method. For the phase-field method, an auxiliary parameter, which varies smoothly across the diffusive phase interface, is used to track the solid-liquid interface implicitly [116, 117]. Unfortunately, the extremely finer grids are indispensable in the interfacial region, which increases the computational effort. In addition, Huang and Wu developed the immersed boundary-thermal lattice Boltzmann method for modeling the solid-liquid phase change phenomenon [118]. The melting interface is explicitly tracked by the Lagrangian grids, and the temperature and fluid flow are solved on the Eulerian nodes. However, an interpolation between the Lagrangian nodes and the Eulerian nodes should be carried out using the Dirac delta function, which reduces the computation accuracy. Compared with other methods, the enthalpy-based method becomes attractive for solid-liquid phase change due to its high efficiency and robustness. Jiang et al. first used LBM with enthalpy formulation to investigate the phase change problems [119]. However, the convective heat transfer is not considered in this work. Huber et al. developed a LBM model using double distribution functions to simulate the solid-liquid phase change process with convective heat transfer [120], and the numerical results are analyzed and compared with scaling laws and previous numerical work. Eshraghi and Felicelli developed an implicit LBM scheme to investigate the conduction with phase change [121]. Different from the previous enthalpy-based LBM, the iteration of nonlinear latent heat source term in the energy equation is avoided by solving a linear system of equations. Feng et al. further extended this implicit model with a consideration of natural convection to investigate the melting process of nanoparticle-enhanced PCMs [122]. To improve the computational efficiency, Huang et al. modified the equilibrium distribution function of temperature for enthalpy, so that the iteration of heat source term or solving a linear system of equations is not indispensable [123]. Unfortunately, the stability range of relaxation time for this model is narrow, which limits its applications for real scientific and engineering problems. To handle this drawback, Huang and Wu improved their work by using a multiple-relaxation-time (MRT) collision scheme instead of the single-relaxation-time (SRT) one, so that the numerical stability is highly ameliorated [124]. In addition, the thermal conductivity and the specific heat capacity are decoupled from the relaxation time and equilibrium distribution

function, which make this model appropriate for satisfying the Dirichlet-Neumann boundary conditions for conjugate heat transfer. As the model developed by Huang et al. is limited in two-dimensional cases, Li et al. recently developed the SRT and MRT models for axisymmetric and three-dimensional solid-liquid phase change problems [125, 126]. Besides, to speed up the computation, Su and Davidson worked out a mesoscopic scale timestep adjustable non-dimensional LBM [127], and the time steps can be adjusted independent of mesh size by changing the transient mesoscopic Mach number. Furthermore, although the key advantage of LBM is to carry out the pore-scale numerical modeling of heat transfer in porous media, a few lattice Boltzmann models for solid-liquid phase change in porous media at the representative elementary volume (REV) scale are also developed [128–130]. The classical enthalpy-based MRT lattice Boltzmann model developed by Huang and Wu is reviewed in this section because of its simplicity and wide application by researchers for latent heat thermal energy storage problems.

3.2 Multiple-relaxation-time (MRT) method

3.2.1 MRT LBM for fluid flow

The general two dimensional nine-velocity (D2Q9) MRT LBM model is presented in this part for simulating the fluid flow. In the D2Q9 model, lattice velocities \mathbf{e}_i are given by:

$$\mathbf{e}_i = \begin{cases} \mathbf{e}_0 = (0, 0) \\ \mathbf{e}_i = c(\cos[(i-1)\pi/2], \sin[(i-1)\pi/2]), & i = 1, 2, 3, 4 \\ \mathbf{e}_i = \sqrt{2}c(\cos[(2i-9)\pi/4], \sin[(2i-9)\pi/4]), & i = 5, 6, 7, 8 \end{cases} \quad (19)$$

where c is the lattice speed, and the collision step carried out in the momentum space is given as:

$$\mathbf{m}_f(\mathbf{x}, t + \delta_t) = \mathbf{m}_f(\mathbf{x}, t) - \mathbf{S}[\mathbf{m}_f(\mathbf{x}, t) - \mathbf{m}_f^{eq}(\mathbf{x}, t)] + \delta_t \left(\mathbf{I} - \frac{\mathbf{S}}{2} \right) \mathbf{F}_m(\mathbf{x}, t) \quad (20)$$

where \mathbf{x} is the location vector, t is the time, δ_t is the time step, \mathbf{I} is the unit matrix, and \mathbf{m}_f is the distribution function in momentum space defined as:

$$\mathbf{m}_f(\mathbf{x}, t) = [m_{f0}(\mathbf{x}, t), m_{f1}(\mathbf{x}, t), \dots, m_{f8}(\mathbf{x}, t)]^T \quad (21)$$

The equilibrium distribution function in momentum space \mathbf{m}_f^{eq} is [131–133]:

$$\mathbf{m}_f^{eq} = \left(\rho, -2\rho + 3\rho \frac{|\mathbf{u}|^2}{c^2}, \rho - 3\rho \frac{|\mathbf{u}|^2}{c^2}, \rho \frac{u_x}{c}, -\rho \frac{u_x}{c}, \rho \frac{u_y}{c}, -\rho \frac{u_y}{c}, \rho \frac{u_x^2 - u_y^2}{c^2}, \rho \frac{u_x u_y}{c^2} \right)^T \quad (22)$$

where ρ is the density, \mathbf{u} is the fluid velocity vector, u_x is the horizontal velocity, and u_y is the vertical velocity. The diagonal relaxation matrix \mathbf{S} is defined as:

$$\mathbf{S} = \text{diag}(s_0, s_e, s_\varepsilon, s_j, s_q, s_j, s_q, s_p, s_p) \quad (23)$$

where $s_0, s_e, s_\varepsilon, s_j, s_q$, and s_p are the parameters related to relaxation time, which could be chosen as described in Ref. [134]. The discrete force term in the momentum space $\mathbf{F}_m(\mathbf{x}, t)$ is given by [135, 136]:

$$\mathbf{F}_m(\mathbf{x}, t) = \left(0, 6 \frac{\mathbf{F} \cdot \mathbf{u}}{c^2}, -6 \frac{\mathbf{F} \cdot \mathbf{u}}{c^2}, \frac{F_x}{c}, -\frac{F_x}{c}, \frac{F_y}{c}, -\frac{F_y}{c}, 2 \frac{F_x u_x - F_y u_y}{c^2}, \frac{F_x u_y + F_y u_x}{c^2} \right)^T \quad (24)$$

where \mathbf{F} is the body force of fluid flow, F_x is the body force in the horizontal direction, and F_y is the body force in the vertical direction. After the collision process, the post collision distribution function in the velocity space $f_i(\mathbf{x}, t + \delta_t)$ is calculated through inverse transformation:

$$f_i(\mathbf{x}, t + \delta_t) = \mathbf{M}^{-1} \mathbf{m}_f(\mathbf{x}, t + \delta_t) \quad (25)$$

where the dimensionless orthogonal transformation matrix \mathbf{M} is chosen as [137]:

$$\mathbf{M} = \begin{Bmatrix} 1 & 1 & 1 & 1 & 1 & 1 & 1 & 1 & 1 \\ -4 & -1 & -1 & -1 & -1 & 2 & 2 & 2 & 2 \\ 4 & -2 & -2 & -2 & -2 & 1 & 1 & 1 & 1 \\ 0 & 1 & 0 & -1 & 0 & 1 & -1 & -1 & 1 \\ 0 & -2 & 0 & 2 & 0 & 1 & -1 & -1 & 1 \\ 0 & 0 & 1 & 0 & -1 & 1 & 1 & -1 & -1 \\ 0 & 0 & -2 & 0 & 2 & 1 & 1 & -1 & -1 \\ 0 & 1 & -1 & 1 & -1 & 0 & 0 & 0 & 0 \\ 0 & 0 & 0 & 0 & 0 & 1 & -1 & 1 & -1 \end{Bmatrix} \quad (26)$$

Then, the streaming step is carried out as:

$$f_i(\mathbf{x} + \mathbf{e}_i \delta_t, t + \delta_t) = f_i(\mathbf{x}, t + \delta_t) \quad (27)$$

The nonslip velocity condition on the diffusive interface and in the solid phase is tackled by recalculating the density distribution function f_i through a linear interpolation as [138]:

$$f_i = f_l f_i + (1 - f_l) f_i^{eq}(\rho, \mathbf{u}_s) \quad (28)$$

f_l is the liquid fraction of PCM, f_i^{eq} is the equilibrium distribution function, which could be calculated by inverse transformation as $f_i^{eq} = \mathbf{M}^{-1} \mathbf{m}_f^{eq}$. For the solid phase, there is $\mathbf{u}_s = \mathbf{0}$. Hence, the macroscopic variables, density ρ and velocity \mathbf{u} , are defined as:

$$\rho = \sum_{i=0}^8 f_i, \quad \rho \mathbf{u} = \sum_{i=0}^8 \mathbf{e}_i f_i + \frac{\delta_t}{2} \mathbf{F} \quad (29)$$

As mentioned in Ref. [138], the density ρ in the term $f_i^{eq}(\rho, \mathbf{u}_s)$ in Eq. (28) should be first calculated by Eq. (29) in order to ensure the mass conservation. Then, for the liquid phase of $f_l = 1$, the above lattice Boltzmann model recovers to the standard scheme for incompressible flow. On the other hand, for the solid phase of $f_l = 0$, the above model could satisfy that $f_i = f_i^{eq}(\rho, \mathbf{u}_s)$ indicating that the nonslip velocity $\mathbf{u} = \mathbf{u}_s$ is ensured.

3.2.2 MRT LBM for solid-liquid phase change

The MRT lattice Boltzmann equation (LBE) for the total enthalpy H distribution function $\mathbf{m}_g(\mathbf{x}, t)$ is expressed as [124]:

$$\mathbf{m}_g(\mathbf{x}, t + \delta_t) = \mathbf{m}_g(\mathbf{x}, t) - \mathbf{S} \left[\mathbf{m}_g(\mathbf{x}, t) - \mathbf{m}_g^{eq}(\mathbf{x}, t) \right] \quad (30)$$

where \mathbf{m}_g is the distribution in momentum space given as:

$$\mathbf{m}_g(\mathbf{x}, t) = [m_{g0}(\mathbf{x}, t), m_{g1}(\mathbf{x}, t), \dots, m_{g8}(\mathbf{x}, t)]^T \quad (31)$$

The equilibrium moment \mathbf{m}_g^{eq} is given by:

$$\mathbf{m}^{eq} = \left(H, -4H + 2c_{p,ref}T + 3c_pT\frac{u^2}{c^2}, 4H - 3c_{p,ref}T - 3c_pT\frac{u^2}{c^2}, \right. \\ \left. c_pT\frac{u_x}{c}, -c_pT\frac{u_x}{c}, c_pT\frac{u_y}{c}, -c_pT\frac{u_y}{c}, c_pT\frac{u_x^2 - u_y^2}{c^2}, c_pT\frac{u_x u_y}{c^2} \right)^T \quad (32)$$

where T is the temperature, and c_p is the specific heat calculated by interpolation as:

$$c_p = (1 - f_l)c_{p,s} + f_l c_{p,l} \quad (33)$$

$c_{p,s}$ is the specific heat of PCM at solid state, and $c_{p,l}$ is the specific heat of PCM at liquid state. To achieve good numerical stability, the reference specific heat $c_{p,ref}$ is defined by the harmonic mean of $c_{p,s}$ and $c_{p,l}$ as:

$$c_{p,ref} = \frac{2c_{p,s}c_{p,l}}{c_{p,s} + c_{p,l}} \quad (34)$$

The parameters in the diagonal relaxation matrix \mathbf{S} satisfy $s_0 = 1$, $s_e = s_p$, $s_j = \frac{1}{\tau}$, and $0 < s_{e,\epsilon,q} < 2$, where the relaxation time τ is given as:

$$\frac{k}{\rho c_{p,ref}} = c_s^2(\tau - 0.5)\delta_t \quad (35)$$

where k is the thermal conductivity, and $c_s = \frac{c}{\sqrt{3}}$ is the sound speed. To reduce the numerical diffusion, a “magic” relationship is found by Huang and Wu [124] as:

$$\left(\frac{1}{s_e} - \frac{1}{2} \right) \left(\frac{1}{s_j} - \frac{1}{2} \right) = \frac{1}{4} \quad (36)$$

Similar to the computation of fluid flow, the post-collision distribution function in the velocity space g_i could be calculated by inverse transformation as:

$$g_i(\mathbf{x}, t + \delta_t) = \mathbf{M}^{-1} \mathbf{m}_g(\mathbf{x}, t + \delta_t) \quad (37)$$

The streaming process is completed as:

$$g_i(\mathbf{x} + \mathbf{e}_i \delta_t, t + \delta_t) = g_i(\mathbf{x}, t + \delta_t) \quad (38)$$

Then, the enthalpy H is calculated as:

$$H = \sum_{i=0}^8 g_i \quad (39)$$

Furthermore, it should be pointed out that the nonequilibrium extrapolation method developed by Guo et al. could be applied for the boundary conditions of fluid flow and enthalpy on the surfaces of LHTES unit [139, 140].

3.3 Classical examples for code validation

3.3.1 One-dimensional transient conjugate heat transfer

To validate the capability of MRT LBM for tackling the differences in thermophysical properties, the one-dimensional transient conjugate heat transfer in two regions without phase change is used to compare the numerical results with analytical solutions. Initially, T is equal to 1 in the region A at $x > 0$, and T is equal to 0 in the region B at $x < 0$. The analytical solution for this problem is given as [141]:

$$T^A(x, t) = \frac{1}{1 + \sqrt{(\rho C_p)^B k^B / (\rho C_p)^A k^A}} \left[1 + \sqrt{(\rho C_p)^B k^B / (\rho C_p)^A k^A} \operatorname{erf} \left(\frac{x}{2\sqrt{k^A t / (\rho C_p)^A}} \right) \right] \quad (40)$$

$$T^B(x, t) = \frac{1}{1 + \sqrt{(\rho C_p)^B k^B / (\rho C_p)^A k^A}} \operatorname{erfc} \left(-\frac{x}{2\sqrt{k^B t / (\rho C_p)^B}} \right) \quad (41)$$

When the aluminum is used for region A while the liquid water is chosen as the material in region B, the comparison between LBM results and analytical solutions is presented in **Figure 8**. A good agreement is observed, and the maximum L2 error with 200×200 lattice grids is only 6.7983×10^{-5} [142].

3.3.2 One-dimensional melting by conduction

In order to verify the MRT LBM for solid-liquid phase change phenomenon, the one-dimensional melting by conduction at a constant phase change temperature T_m is simulated. Initially, the substance is uniformly solid at a temperature T_0 ($T_0 < T_m$). The melting process begins at time $t = 0$ when the temperature of the left wall is at a high temperature of T_h ($T_h > T_m$). Then, the analytical solution for the temperature in this problem is given as [143]:

$$T(x, t) = T_h - \frac{T_h - T_m}{\operatorname{erf}(\lambda)} \operatorname{erf} \left(\frac{x}{2\sqrt{k_l t / (\rho c_{p,l})}} \right), 0 \leq x \leq X_i(t), \text{ liquid} \quad (42)$$

$$T(x, t) = T_0 + \frac{T_m - T_0}{\operatorname{erfc}(\lambda / \sqrt{R_{ac}})} \operatorname{erfc} \left(\frac{x}{2\sqrt{k_s t / (\rho c_{p,s})}} \right), x > X_i(t), \text{ solid} \quad (43)$$

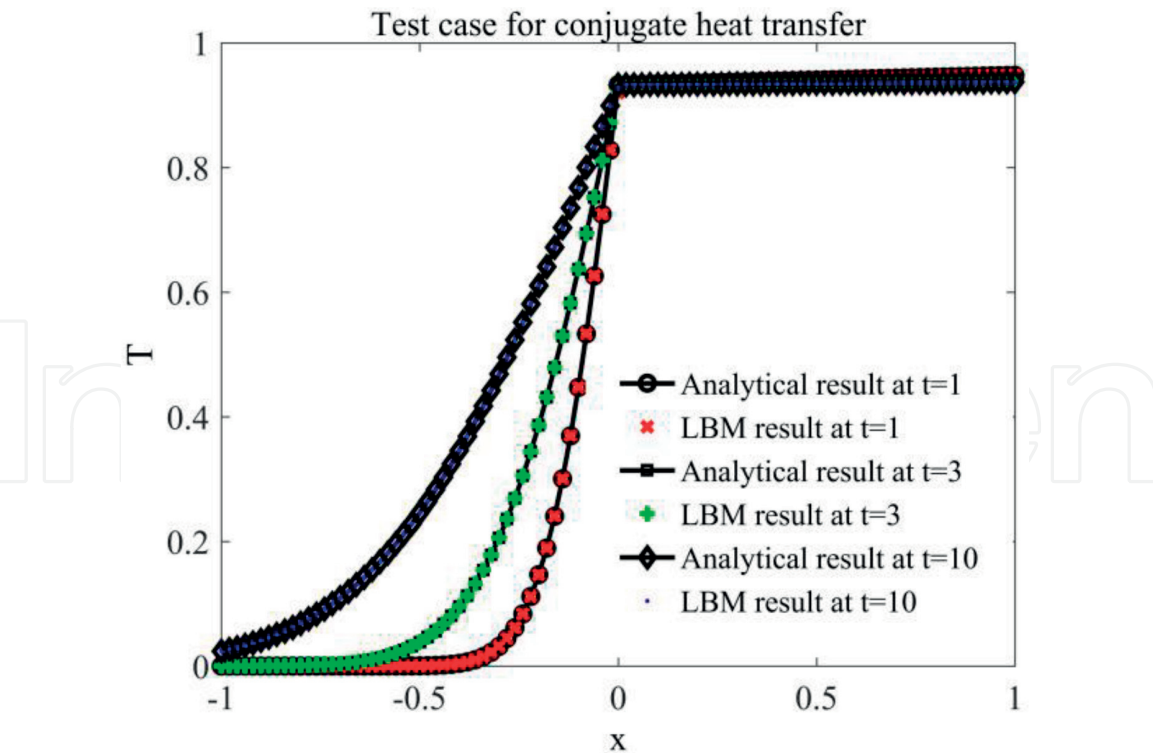


Figure 8.
 One-dimensional transient conjugate heat transfer [142].

where k_l and k_s are the thermal conductivities of liquid PCM and solid PCM, respectively. The parameter $R_{ac} = \frac{[k_s t / (\rho c_{p,s})]}{[k_l t / (\rho c_{p,l})]}$ is the ratio of thermal diffusivity between the solid and liquid phases of PCM, and the location of phase interface X_i is calculated as:

$$X_i = 2\lambda \sqrt{k_l t / (\rho c_{p,l})} \tag{44}$$

The parameter λ is the root of the transcendental equation:

$$\frac{Ste_l}{\exp(\lambda^2)\text{erf}(\lambda)} - \frac{Ste_s \sqrt{R_{ac}}}{\exp(\lambda^2/R_{ac})\text{erfc}(\lambda/\sqrt{R_{ac}})} = \lambda \sqrt{\pi} \tag{45}$$

where the Stefan numbers, Ste_l and Ste_s , are defined as:

$$Ste_l = \frac{c_{p,l}(T_h - T_m)}{L}, Ste_s = \frac{c_{p,s}(T_m - T_0)}{L} \tag{46}$$

The comparison of temperature T between the analytical solutions and the SRT or MRT LBM with different relaxation times is presented in **Figure 9**. It could be observed that the numerical diffusion exists for the small (τ_l close to 0.5) and large ($\tau_l > 2$) relaxation times when the SRT model is applied. However, the numerical diffusion is highly reduced once the MRT model with a “magic” parameter relation shown in Eq. (36) is used.

3.3.3 Two-dimensional melting by convection

The natural convection with melting in a square cavity heated from the side wall is usually used to validate the code for solid-liquid phase change. First, the

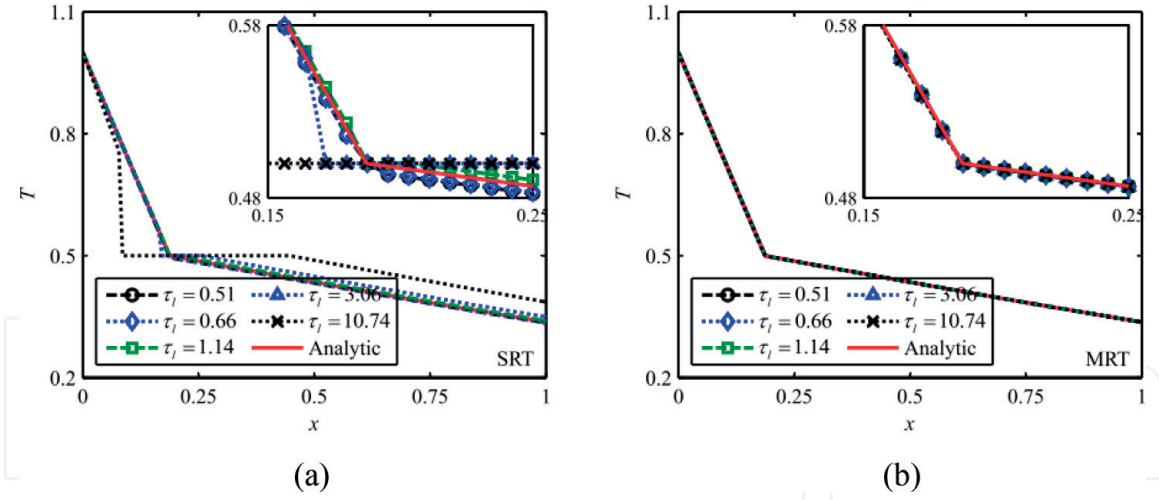


Figure 9. (a) SRT LBM (b) MRT LBM. Comparison of temperature T between analytical solutions and SRT or MRT LBM results with different relaxation times [124].

solid-liquid phase change with convection in a cavity at the Rayleigh number $Ra = 25000$, the Prandtl number $Pr = 0.02$, and the Stefan number $Ste = 0.01$ is compared with the results by Mencinger [144]. The average Nusselt number Nu_{ave} at the hot wall in terms of the Fourier numbers Fo is plotted in **Figure 10(a)**, and the melting interface positions at $Fo = 10$ and $Fo = 20$ are shown in **Figure 10(b)**. In addition, the average melting fraction f_l is also presented in **Figure 10(c)**. It is

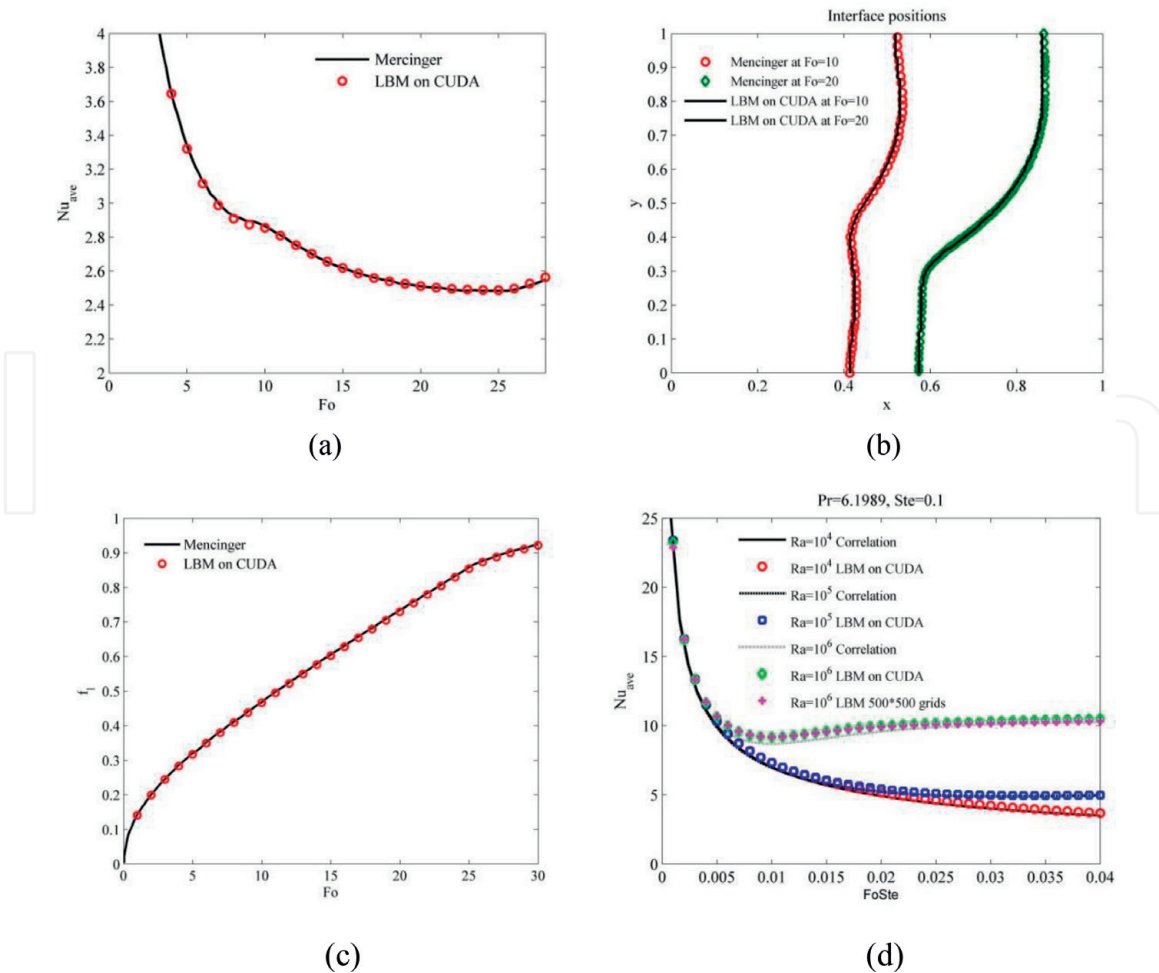


Figure 10. Natural convection with melting in a cavity [142].

obvious that the current LBM results are consistent with the work of Mencinger [142]. Besides, for the cases of $Pr > 1$, the MRT LBM for natural convection with melting in cavity could be calibrated by the scaling laws and correlations derived by Jany and Bejan [145]. The average Nusselt number Nu_{ave} at hot wall is given as:

$$Nu_{ave} = (2FoSte)^{-1/2} + \left[0.33Ra^{1/4} - (2FoSte)^{-1/2} \right] \left\{ 1 + \left[0.0175Ra^{3/4}(FoSte)^{3/2} \right]^{-2} \right\}^{-1/2} \tag{47}$$

As shown in **Figure 10(d)**, the average Nusselt number Nu_{ave} at $Pr = 6.1989$ and $Ste = 0.1$ agrees well with the results of scaling law correlations at different Rayleigh number Ra .

3.4 GPU acceleration

The characteristic of highly parallel nature is a significant advantage of LBM over other traditional macroscopic numerical methods. In the CUDA programming platform, the CPU and GPU work as the host and the devices, respectively, as shown in **Figure 11** [146]. It means that the parallel tasks are executed on GPU, while the CPU is responsible for the initial conditions and all the sequential

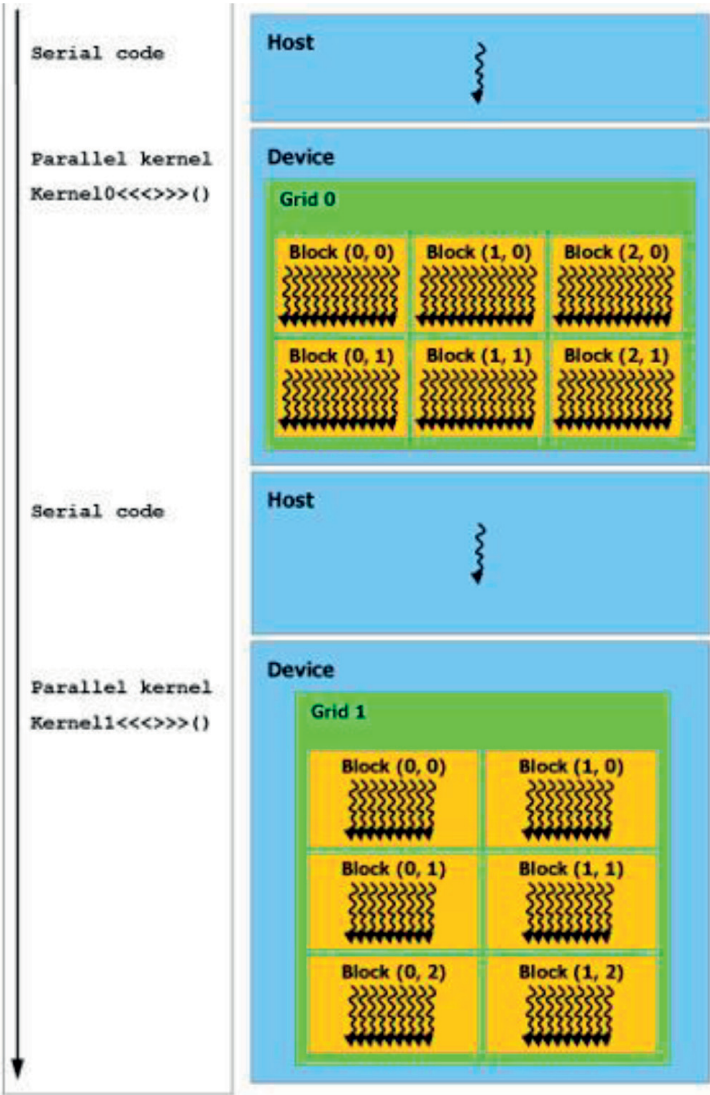


Figure 11.
Schematic diagram of CUDA platform [146].

commands. First, the initial conditions are set up in the host memory, and then the data are moved to the memory of GPU. The threads are grouped into blocks, which are the component of grids as displayed in **Figure 11**. For instance, in the real simulation, if the lattice grid number is (M_x, M_y, M_z) and the block size is (N_x, N_y, N_z) , the corresponding grid size is $(M_x/N_x, M_y/N_y, M_z/N_z)$. Furthermore, a kernel is a function, which is executed on the concurrent threads on GPU. The collision step, streaming step, tackling of boundary conditions, and computation of macroscopic variables are completed in different kernels. It is important to note that all the kernels should be synchronized between CPU and GPU. Finally, the data on the GPU should be copied to the host memory of CPU for printing at any specific time when the results are needed. During the recent years, LBM is demonstrated to be appropriate for GPU computing [147–151], and it has been applied to solve several different physical problems [152–155].

4. Applications of LBM modeling in latent heat thermal energy storage

4.1 Enhancement of PCM performance with fins

As presented in the previous sections, the extended fins could be used to increase the heat transfer depth in LHTES system and accelerate the energy storage efficiency. In the recent years, LBM is applied by several researches to study the solid-liquid phase change of PCMs with extended fins [142, 156, 157]. Jourabian et al. studied the melting process of PCM in a cavity with a horizontal fin heated from the sidewall by enthalpy-based D2Q5 LBM [156]. The results indicated that adding a fin enhances the melting rate for all positions and different lengths compared with the LHTES cavity without fin. They also found that although varying the position of the fin from the bottom to the middle has a negligible effect on melting rate, the melting time is increased once the fin is mounted on the top of LHTES cavity. Talati and Taghilou used an implicit LBM to study the PCM solidification in a rectangular finned container [157]. It was found that the optimum aspect ratio of container for solidification equals to 0.5, and changing the fin material from aluminum to copper has no significant influence on the solidification rate. Ren and Chan applied enthalpy-based MRT LBM to investigate the PCM melting performance in an enclosure with internal fins and finned thick walls with GPU acceleration [142]. The transient PCM melting process with different number of fins at the Fourier number $Fo = 0.15$ is shown in **Figure 12** in terms of temperature contours, liquid fraction, and streamlines. It could be found that the PCM melting rate is obviously enhanced by adding more internal fins in the cavity. However, the energy storage capacity of LHTES system is reduced when the number of internal fins increases, so that the appropriate fin configuration and number should be designed for engineering applications. They found that using a less number of longer fins is more effective than applying shorter fins for enhancing the thermal performance of PCMs. Besides, compared with the LHTES cavity with horizontal fins heated from side walls, the LHTES enclosure using vertical fins heated from the bottom surface has a better charging rate. From the above researches, it should be concluded that the enthalpy-based LBM is successful for simulating the conjugate heat transfer with solid-liquid phase change for melting and solidification of PCMs accelerated with fins.

4.2 Nanoparticle-enhanced PCM

The nanoparticles are commonly used to ameliorate the low thermal conductivity of most PCMs. With some appropriate assumptions as presented in Section 2,

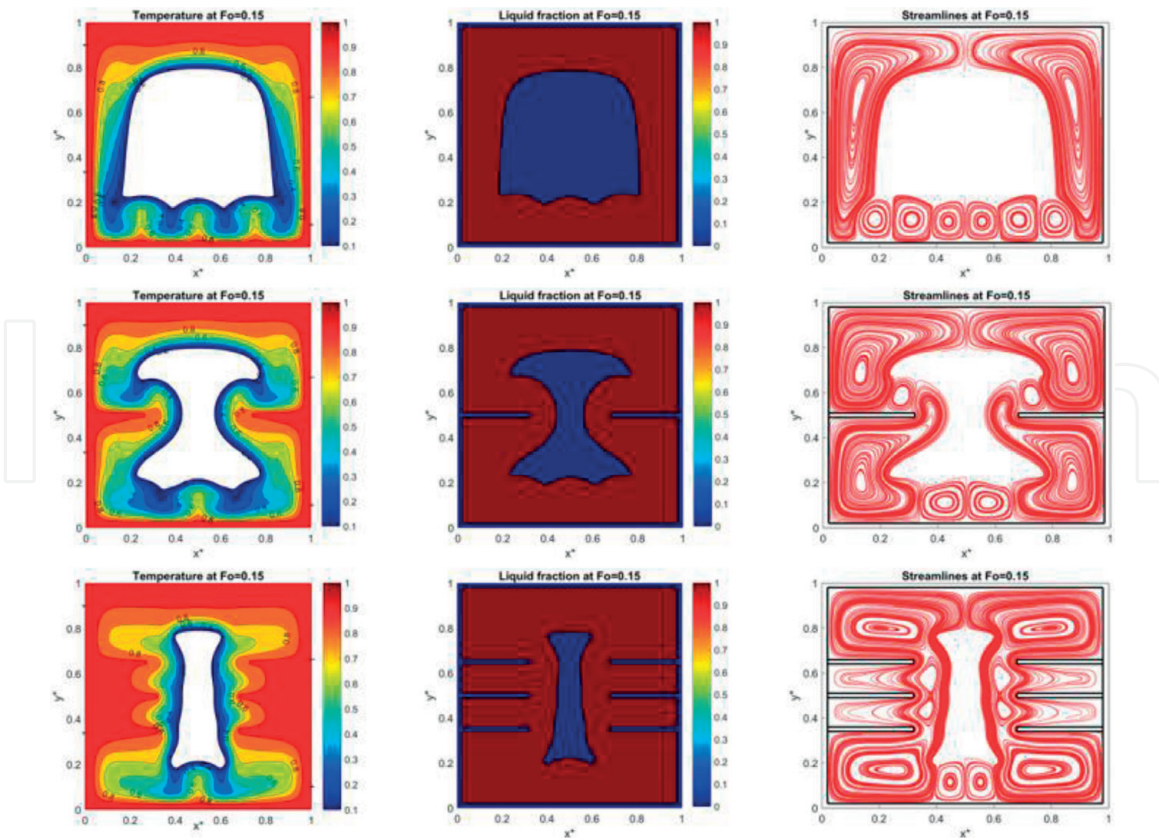


Figure 12.
 Transient PCM melting process with different number of fins [142].

the thermal performance of PCMs with nanoparticles could be modeled using enthalpy-based LBM. Jourabian et al. studied the convective melting process of Cu-nanoparticle enhanced water-ice in a cylindrical-horizontal annulus [158, 159]. It was demonstrated that the melting rate of NEPCM is accelerated due to the improvement of thermal conductivity and the reduced latent heat. When the heated cylinder located in the bottom section of the annulus, the increment effect on NEPCM melting rate by adding more nanoparticles decreases because of the augmentation of NEPCM viscosity, which weakens the convective heat transfer. Feng et al. investigated the melting of water (ice)-copper nanoparticle NEPCM in a bottom-heated rectangular cavity by treating the latent heat source term with an implicit scheme [122]. They also found that the heat transfer rate of NEPCM increases with respect to the increment of nanoparticle volume fractions. However, the energy storage rate is the most significant parameter for a LHTES unit. Although adding nanoparticles into PCMs could increase their thermal conductivity, it increases the viscosity of PCM, which weakens the convective heat transfer. Due to this reason, the energy storage rate of LHTES system may even decrease with the increasing nanoparticle volume fractions, especially for the case with large temperature gradient. On the other hand, the increment of nanoparticle volume fraction decreases the energy storage capacity of LHTES unit, so that the energy storage rate could also be affected. Under this circumstance, more future research attentions should be paid on the influences of nanoparticles on the energy storage rate of NEPCM. In addition, the solid-liquid phase change model of NEPCM using LBM could be extended to study the charging and discharging of NEPCM under hybrid heat transfer enhancement techniques such as nanoparticle-fin or nanoparticle-metal foam combinations.

4.3 PCM filled with metal foams

Due to its intersected and connected heat transfer channels, metal foam is inserted into the LHTES system for enhancing the melting and solidification rates of PCMs. The numerical modeling of PCM solid-liquid phase change phenomenon filled in metal foams using enthalpy-based LBM could be categorized as the representative elementary volume (REV) scale modeling [128–130, 160] and pore-scale modeling [111, 161]. Tao et al. investigated the performance of metal foams/paraffin composite PCM in a LHTES cavity using LBM at REV scale [160]. They found that increasing the metal foam PPI (number of pores per inch) could enhance the conduction heat transfer, while the convective heat transfer is weakened. In addition, although decreasing the metal foam porosity could accelerate the PCM melting rate, the energy storage density of LHTES unit is dramatically reduced. Due to the above two tradeoffs, the optimum metal foam structure with the porosity of 0.94 and PPI of 45 is highly recommended. However, the REV scale modeling requires the use of some empirical relations, and the influences of metal foam morphology on energy storage rate are difficult to be analyzed. As a comparison, with the advantage of

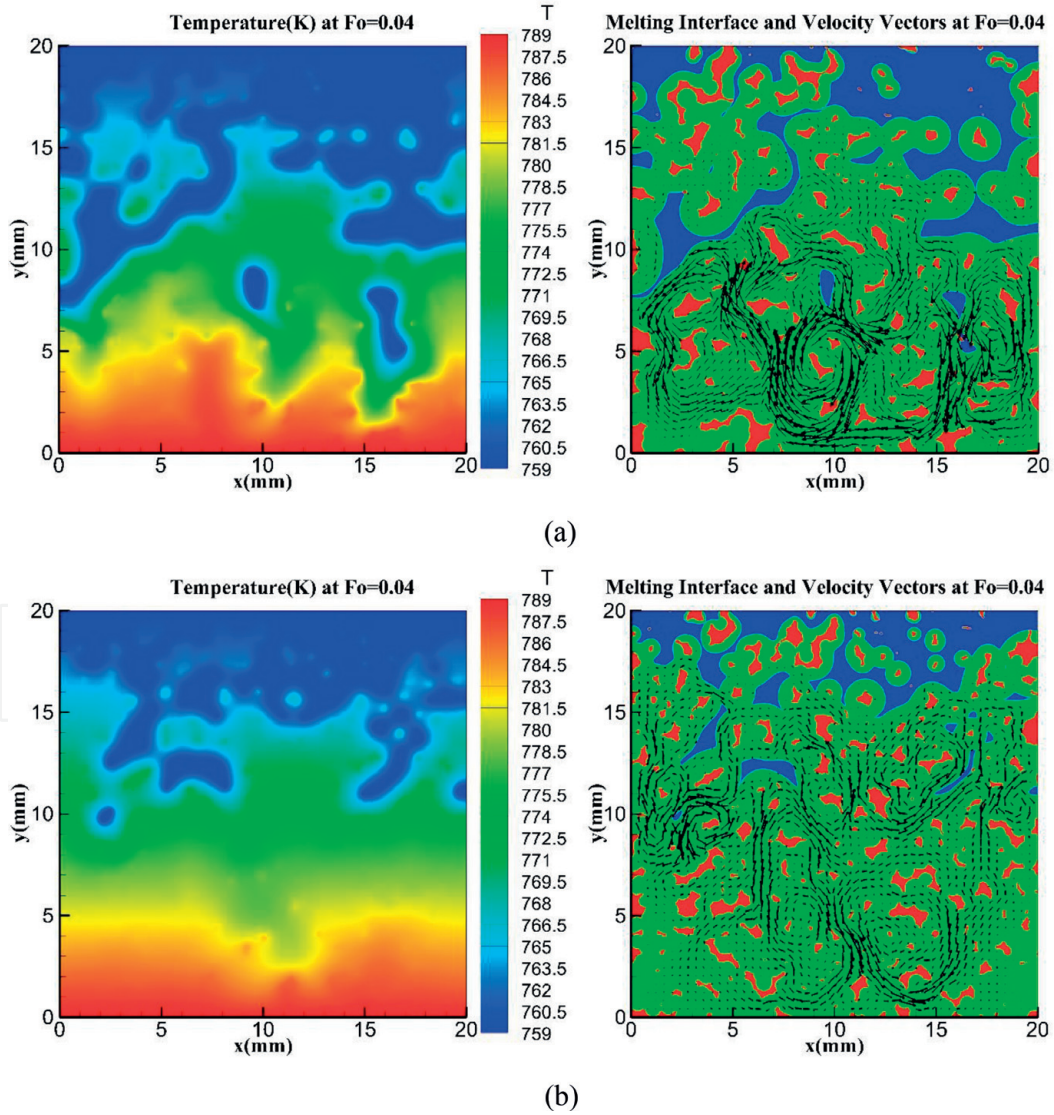


Figure 13. Transient PCM melting process filled in metal foams with different pore sizes [111]. (a) $\epsilon_{ave} = 0.95$ and $d_p = 1$ mm and (b) $\epsilon_{ave} = 0.95$ and $d_p = 0.75$ mm.

LBM for tackling complex boundary conditions, pore-scale modeling without using any empirical equations achieves the detailed fluid flow and heat transfer information inside the metal foams, so that the energy storage efficiency of LHTES unit could be further optimized. Ren et al. investigated the effects of metal foam characteristics on the PCM melting rate through pore-scale LBM modeling [111]. The transient PCM melting process inside the metal foams of different pore sizes at the Fourier number $Fo = 0.04$ is plotted with respect to temperature field, melting interface, and fluid velocity vectors in **Figure 13**. It could be observed that the charging rate of PCM is accelerated when the pore size decreases from $d_p = 1 \text{ mm}$ to $d_p = 0.75 \text{ mm}$ at a porosity of $\varepsilon_{ave} = 0.95$. Furthermore, the temperature field in the melted region of LHTES with smaller pore size $d_p = 0.75 \text{ mm}$ is found to be more uniform than that of LHTES with pore size $d_p = 1.0 \text{ mm}$, which means that the thermal conductivity and its corresponding conduction heat transfer in LHTES unit are improved with a decreasing pore size (increasing PPI). Besides, they also concluded that an appropriate metal foam porosity should be chosen in the real engineering applications in order to balance the PCM melting speed and the energy storage density of LHTES unit. By reconstructing the microstructure of metal foam with X-ray computed tomography, Li et al. investigated the solid-liquid phase change phenomenon of PCM inserted with metal foams under different gravitational acceleration conditions [161]. The results indicated that the transition of the dominant heat transfer mechanism from convection to conduction occurs when the gravity gradually decreases. Due to the attenuated convection effect with decreasing gravity, the PCM melting development is dramatically hindered. Besides, they also concluded that the decreasing metal foam porosity could enhance the effective thermal conductivity of LHTES unit because of the extended heat transfer area. However, the above pore-scale modeling of PCM charging and discharging processes enhanced by metal foams is limited in two-dimensional cases. The three-dimensional pore-scale modeling, which is indispensable for optimizing the complicated metal foam structures, should be carried out in the future work.

4.4 PCM with heat pipes

The heat pipes are used to transfer heat between PCMs and heat transfer fluid (HTF), so that the charging and discharging of LHTES system could be accelerated. The configuration, arrangement, and number of heat pipes in the LHTES unit are essential for the PCM melting and solidification speed. Luo et al. applied LBM to study the convection melting in complex LHTES system with heat tubes [162]. The effects of inner heat pipe arrangement on PCM melting process are illustrated in **Figure 14** with respect to temperature, flow, and phase fields at the Fourier number $Fo = 3$, the Prandtl number $Pr = 0.2$, the Stefan number $Ste = 0.02$, and the Rayleigh number $Ra = 5 \times 10^4$. For the case using centrosymmetric inner heat pipes, the conduction heat transfer is dominant because the inner heat pipe is surrounded by solid PCM at the melting temperature, so that its melting rate is faster than the LHTES system with inline or staggered heat tubes as displayed in **Figure 15**. In addition, there is no obvious difference between the melting rates of LHTES systems using inline or staggered heat pipes. Although using heat pipe individually could enhance the thermal performance of LHTES to some extent, other heat transfer enhancement techniques are usually coupled with heat pipes such as fins or nanoparticles to further improve the PCM charging and discharging rate.

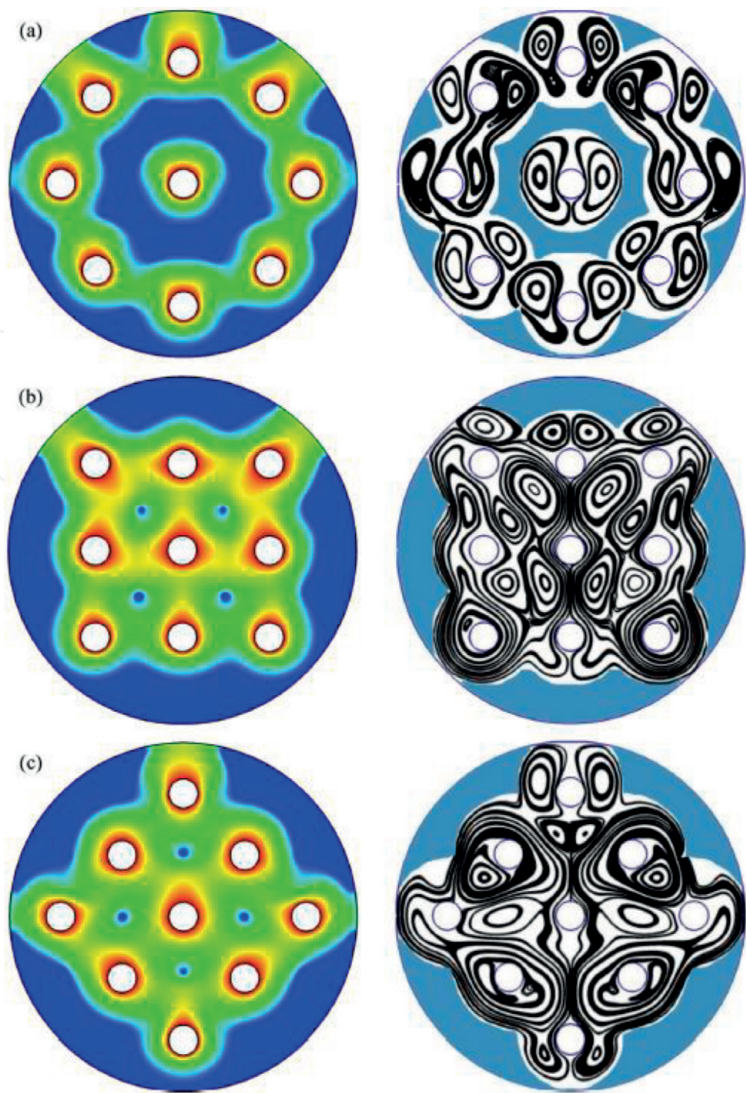


Figure 14. Temperature, flow, and phase fields at $Fo = 3$ with different arrangements of inner tubes: (a) centrosymmetric, (b) inline, and (c) staggered for the Prandtl number $Pr = 0.2$, the Stefan number $Ste = 0.02$, and the Rayleigh number $Ra = 5 \times 10^4$ [162].

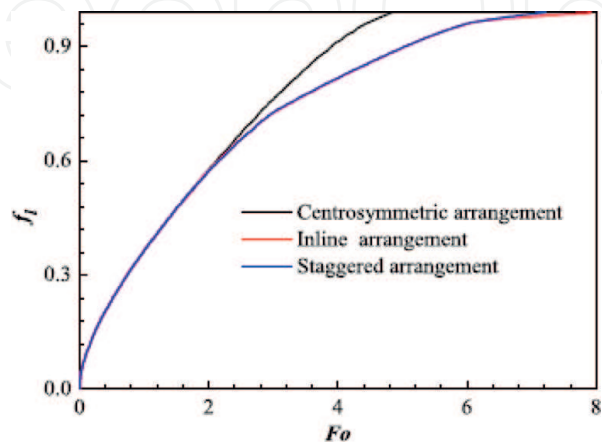


Figure 15. The total liquid fraction f_l versus the Fourier number Fo for different arrangements of inner tubes at the Prandtl number $Pr = 0.2$, the Stefan number $Ste = 0.02$, and the Rayleigh number $Ra = 5 \times 10^4$ [162].

4.5 PCM with hybrid heat transfer enhancement techniques

In this section, the melting and solidification of PCMs enhanced using combined heat transfer enhancement techniques modeled by LBM are discussed, and the effectiveness of different approaches for improving the heat transfer capability of LHTES unit is compared. Huo and Rao carried out an investigation of NEPCM solid-liquid phase change process in a cavity with a heat pipe and separate plates using LBM [163]. It was found that the NEPCM of the case with separate located in the middle of cavity melts fastest because of the weakened heat accumulation. The results also showed that when the location of separate is less than 0.3, the melting rate of NEPCM is even slowed down due to the heat accumulation around the separate plate. Gao et al. developed an enthalpy-based MRT LBM model with a free parameter in the equilibrium distribution function for solid-liquid phase change in porous media and conjugate heat transfer with high-computational efficiency and stability [164]. Then, they investigated the PCM melting process in porous media with a conducting fin, and the results indicated that the heat transfer rate could be further improved by adding a fin into the porous medium. It was also observed that the vertical position of the fin has no remarkable impact on the PCM melting speed when there exists porous media. Jourabian et al. investigated the constrained ice melting around a cylinder using three heat transfer enhancement techniques by LBM [165]. They pointed out that adding nanoparticles may increase the dynamic viscosity of the base PCM, which

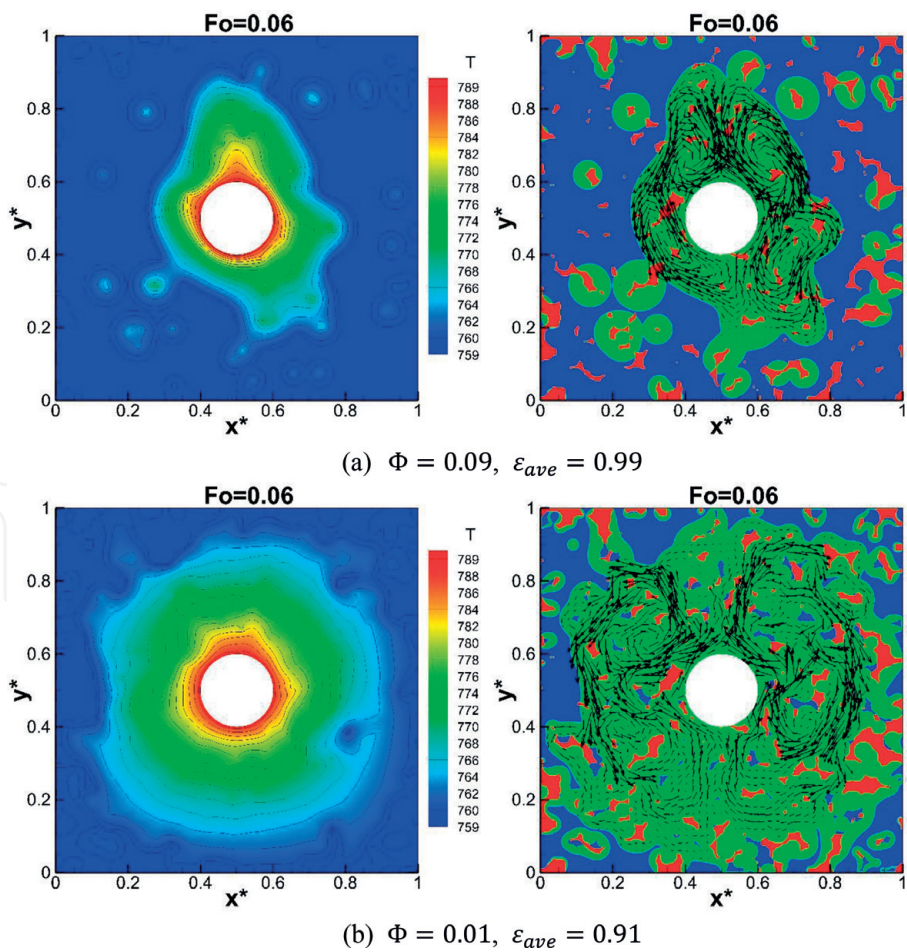


Figure 16. Transient nanoparticle-enhanced PCM melting process filled in metal foams of pore size $d_p = 1$ mm and heat pipe radius $R = 2$ mm [166]. (a) $\Phi = 0.09, \epsilon_{ave} = 0.99$ and (b) $\Phi = 0.01, \epsilon_{ave} = 0.91$.

has a negative effect on natural convective heat transfer. Besides, the tradeoff between consolidating the conduction heat transfer and weakening the convective heat transfer through decreasing the metal foam porosity needs further attention and investigation. Ren et al. completed a pore-scale comparative study of nanoparticle-enhanced PCM melting in a heat pipe-assisted LHTES unit with metal foams [166]. The melting process of NEPCM in a LHTES cavity filled with metal foams using a heat pipe at the Fourier number $Fo = 0.06$, pore size $d_p = 1 \text{ mm}$, and heat pipe radius $R = 2 \text{ mm}$ is shown in **Figure 16**. Although different combinations of nanoparticle volume fraction Φ and metal foam porosity ε_{ave} are used for the LHTES unit, it should be noted that the volume fraction of pure PCM is kept at 90%, so that the energy storage capacity is unchanged for a fair comparison. It could be observed that the NEPCM with less nanoparticle volume fraction and lower metal foam porosity melts faster than that with more nanoparticles in the higher porosity metal foam. This finding indicated that using metal foams is more effective than adding nanoparticles for enhancing the charging rate of NEPCMs. They also found that there exists an optimum heat pipe radius for achieving the best energy storage rate in LHTES unit. As discussed in the above sections, LBM is demonstrated to be appropriate for simulating the charging and discharging processes of PCMs in LHTES system with different kinds of heat transfer enhancement technologies. Under this circumstance, the enthalpy-based LBM will definitely play a more significant role in the future research of thermal energy storage using PCMs.

5. Summary

In this chapter, different heat transfer enhancement techniques of PCMs for LHTES unit are discussed and compared. As the numerical modeling plays a significant role in clarifying the mechanism of complicated physical processes, the mathematical models for fluid flow of liquid PCMs and the PCM solid-liquid phase change phenomenon are presented. In order to investigate the PCM charging and discharging processes enhanced by nanoparticles, fins, or metal foams, the empirical relations for nanofluids and the mathematical formula for conjugate heat transfer are shown. The development history of the lattice Boltzmann method for solid-liquid phase change problems is carefully reviewed, and the enthalpy-based multiple-relaxation-time LBM is discussed in detail due to its simplicity and robustness. Besides, the implementation of GPU computing is briefly discussed to accelerate the computational efficiency of LBM modeling. Then, the applications of LBM modeling in LHTES system with different heat transfer enhancement approaches are presented, which demonstrate that the mesoscopic and highly parallel LBM is powerful for understanding the melting and solidification processes of PCMs.

Acknowledgements

This work was financially sponsored by the National Key Research and Development Program of China (No. 2017YFB0102703), the National Natural Science Foundation of China (No. 51536003), 111 Project (grant number B16038), and the Foundation for Innovative Research Groups of the National Natural Science Foundation of China (No. 51721004).

IntechOpen

IntechOpen


Author details

Zhiguo Qu

Key Laboratory of Thermo-Fluid Science Engineering of MOE, School of Energy and Power Engineering, Xi'an Jiaotong University, Xi'an, Shaanxi, China

*Address all correspondence to: zgqu@mail.xjtu.edu.cn

IntechOpen

© 2018 The Author(s). Licensee IntechOpen. This chapter is distributed under the terms of the Creative Commons Attribution License (<http://creativecommons.org/licenses/by/3.0>), which permits unrestricted use, distribution, and reproduction in any medium, provided the original work is properly cited. 

References

- [1] Chen H, Cong TN, Yang W, Tan C, Li Y, Ding Y. Progress in electrical energy storage system: A critical review. *Progress in Natural Science*. 2009;**19**(3): 291-312
- [2] Luo X, Wang J, Dooner M, Clarke J. Overview of current development in electrical energy storage technologies and the application potential in power system operation. *Applied Energy*. 2015; **137**:511-536
- [3] Ibrahim NI, Al-Sulaiman FA, Rahman S, Yilbas BS, Sahin AZ. Heat transfer enhancement of phase change materials for thermal energy storage applications: A critical review. *Renewable and Sustainable Energy Reviews*. 2017;**74**:26-50
- [4] Abdulateef AM, Mat S, Abdulateef J, Sopian K, Al-Abidi AA. Geometric and design parameters of fins employed for enhancing thermal energy storage systems: A review. *Renewable and Sustainable Energy Reviews*. 2018;**82**: 1620-1635
- [5] Sharifi N, Bergman TL, Faghri A. Enhancement of PCM melting in enclosures with horizontally-finned internal surfaces. *International Journal of Heat and Mass Transfer*. 2011;**54**: 4182-4192
- [6] Ye W-B, Zhu D-S, Wang N. Numerical simulation on phase-change thermal storage/release in a plate-fin unit. *Applied Thermal Engineering*. 2011;**31**:3871-3884
- [7] Mosaffa AH, Talati F, Rosen MA, Tabrizi HB. Approximate analytical model for PCM solidification in a rectangular finned container with convective cooling boundaries. *International Communications in Heat and Mass Transfer*. 2012;**39**:318-324
- [8] Mat S, Al-Abidi AA, Sopian K, Sulaiman MY, Mohammad AT. Enhance heat transfer for PCM melting in triplex tube with internal-external fins. *Energy Conversion and Management*. 2013;**74**: 223-236
- [9] Al-Abidi AA, Mat S, Sopian K, Sulaiman MY, Mohammad AT. Numerical study of PCM solidification in a triplex tube heat exchanger with internal and external fins. *International Journal of Heat and Mass Transfer*. 2013;**61**:684-695
- [10] Levin PP, Shitzer A, Hetsroni G. Numerical optimization of a PCM-based heat sink with internal fins. *International Journal of Heat and Mass Transfer*. 2013;**61**:638-645
- [11] Fan L-W, Xiao Y-Q, Zeng Y, Fang X, Wang X, Xu X, et al. Effects of melting temperature and the presence of internal fins on the performance of a phase change material (PCM)-based heat sink. *International Journal of Thermal Sciences*. 2013;**70**:114-126
- [12] Kamkari B, Shokouhmand H. Experimental investigation of phase change material melting in rectangular enclosures with horizontal partial fins. *International Journal of Heat and Mass Transfer*. 2014;**78**:839-851
- [13] Sciacovelli A, Gagliardi F, Verda V. Maximization of performance of a PCM latent heat storage system with innovative fins. *Applied Energy*. 2015; **137**:707-715
- [14] Rathod MK, Banerjee J. Thermal performance enhancement of shell and tube latent heat storage unit using longitudinal fins. *Applied Thermal Engineering*. 2015;**75**:1084-1092
- [15] Pakrouh R, Hosseini MJ, Ranjbar AA, Bahrampoury R. A numerical method for PCM-based pin fin heat sinks optimization. *Energy Conversion and Management*. 2015;**103**:542-552

- [16] Jmal I, Baccar M. Numerical study of PCM solidification in a finned tube thermal storage including natural convection. *Applied Thermal Engineering*. 2015;**84**:320-330
- [17] Kalbasi R, Salimpour MR. Constructal design of horizontal fins to improve the performance of phase change material rectangular enclosures. *Applied Thermal Engineering*. 2015;**91**: 234-244
- [18] Yuan Y, Cao X, Xiang B, Du Y. Effect of installation angle of fins on melting characteristics of annular unit for latent heat thermal energy storage. *Solar Energy*. 2016;**136**:365-378
- [19] Eslamnezhad H, Rahimi AB. Enhance heat transfer for phase-change materials in triplex tube heat exchanger with selected arrangements of fins. *Applied Thermal Engineering*. 2017;**113**: 813-821
- [20] Mahdi JM, Lohrasbi S, Ganji DD, Nsofor EC. Accelerated melting of PCM in energy storage systems via novel configuration of fins in the triplex-tube heat exchanger. *International Journal of Heat and Mass Transfer*. 2018;**124**: 663-676
- [21] Ji C, Qin Z, Low Z, Dubey S, Choo FH, Duan F. Non-uniform heat transfer suppression to enhance PCM melting by angled fins. *Applied Thermal Engineering*. 2018;**129**:269-279
- [22] Zhao CY. Review on thermal transport in high porosity cellular metal foams with open cells. *International Journal of Heat and Mass Transfer*. 2012;**55**:3618-3632
- [23] Xiao X, Zhang P, Li M. Preparation and thermal characterization of paraffin/metal foam composite phase change material. *Applied Energy*. 2013; **112**:1357-1366
- [24] Feng S, Zhang Y, Shi M, Wen T, Lu TJ. Unidirectional freezing of phase change materials saturated in open-cell metal foams. *Applied Thermal Engineering*. 2015;**88**:315-321
- [25] Zhao CY, Wu ZG. Heat transfer enhancement of high temperature thermal energy storage using metal foams and expanded graphite. *Solar Energy Materials & Solar Cells*. 2011;**95**: 636-643
- [26] Tian Y, Zhao CY. A numerical investigation of heat transfer in phase change materials (PCMs) embedded in porous metals. *Energy*. 2011;**36**: 5539-5546
- [27] Li WQ, Qu ZG, He YL, Tao WQ. Experimental and numerical studies on melting phase change heat transfer in open-cell metallic foams with paraffin. *Applied Thermal Engineering*. 2012;**37**: 1-9
- [28] Zhou D, Zhao CY. Experimental investigations on heat transfer in phase change materials (PCMs) embedded in porous materials. *Applied Thermal Engineering*. 2011;**31**:970-977
- [29] Cui HT. Experimental investigation on the heat charging process by paraffin filled with high porosity copper foam. *Applied Thermal Engineering*. 2012;**39**: 26-28
- [30] Qu ZG, Li WQ, Wang JL, Tao WQ. Passive thermal management using metal foam saturated with phase change material in a heat sink. *International Communications in Heat and Mass Transfer*. 2012;**39**:1546-1549
- [31] Tian Y, Zhao CY. Thermal and exergetic analysis of metal foam-enhanced cascaded thermal energy storage (MF-CTES). *International Journal of Heat and Mass Transfer*. 2013;**58**:86-96
- [32] Baby R, Balaji C. Experimental investigations on thermal performance enhancement and effect of orientation on porous matrix filled PCM based heat

sink. *International Journal of Communications in Heat and Mass Transfer*. 2013;**46**:27-30

[33] Liu Z, Yao Y, Wu H. Numerical modelling for solid-liquid phase change phenomena in porous media: Shell-and-tube type latent heat thermal energy storage. *Applied Energy*. 2013;**112**: 1222-1232

[34] Chen Z, Gao D, Shi J. Experimental and numerical study on melting of phase change materials in metal foams at pore scale. *International Journal of Heat and Mass Transfer*. 2014;**72**: 646-655

[35] Sundarram SS, Li W. The effect of pore size and porosity on thermal management performance of phase change material infiltrated microcellular metal foams. *Applied Thermal Engineering*. 2014;**64**:147-154

[36] Xiao X, Zhang P, Li M. Effective thermal conductivity of open-cell metal foams impregnated with pure paraffin for latent heat storage. *International Journal of Thermal Sciences*. 2014;**81**: 94-105

[37] Mancin S, Diani A, Doretto L, Hooman K, Rossetto L. Experimental analysis of phase change phenomenon of paraffin waxes embedded in copper foams. *International Journal of Thermal Sciences*. 2015;**90**:79-89

[38] Deng Z, Liu X, Zhang C, Huang Y, Chen Y. Melting behaviors of PCM in porous metal foam characterized by fractal geometry. *International Journal of Heat and Mass Transfer*. 2017;**113**: 1031-1042

[39] Zhang P, Meng ZN, Zhu H, Wang YL, Peng SP. Melting heat transfer characteristics of a composite phase change material fabricated by paraffin and metal foam. *Applied Energy*. 2017;**185**:1971-1983

[40] Zhang Z, Cheng J, He X. Numerical simulation of flow and heat transfer in composite PCM on the basis of two different models of open-cell metal foam skeletons. *International Journal of Heat and Mass Transfer*. 2017;**112**: 959-971

[41] Yang X, Feng S, Zhang Q, Chai Y, Jin L, Lu TJ. The role of porous metal foam on the unidirectional solidification of saturating fluid for cold storage. *Applied Energy*. 2017;**194**:508-521

[42] Esapour M, Hamzehnezhad A, Rabienataj Darzi AA, Jourabian M. Melting and solidification of PCM embedded in porous metal foam in horizontal multi-tube heat storage system. *Energy Conversion and Management*. 2018;**171**:398-410

[43] Zhu Z-Q, Huang Y-K, Hu N, Zeng Y, Fan L-W. Transient performance of a PCM-based heat sink with a partially filled metal foam: Effects of the filling height ratio. *Applied Thermal Engineering*. 2018;**128**:966-972

[44] Zheng H, Wang C, Liu Q, Tian Z, Fan X. Thermal performance of copper foam/paraffin composite phase change material. *Energy Conversion and Management*. 2018;**157**:372-381

[45] Ji H, Sellan DP, Pettes MT, Kong X, Ji J, Shi L, et al. Enhanced thermal conductivity of phase change materials with ultrathin-graphite foams for thermal energy storage. *Energy & Environmental Science*. 2014;**7**: 1185-1192

[46] Li M. A nano-graphite/paraffin phase change material with high thermal conductivity. *Applied Energy*. 2013;**106**:25-30

[47] Alshaer WG, Nada SA, Rady MA, Le Bot C, Palomo Del Barrio E. Numerical investigation of using carbon foam/PCM/nano carbon tubes composites in thermal management of electronic

equipment. *Energy Conversion and Management*. 2015;**89**:873-884

[48] Zou D, Ma X, Liu X, Zheng P, Hu Y. Thermal performance enhancement of composite phase change materials (PCM) using graphene and carbon nanotubes as additives for the potential application in lithium-ion power battery. *International Journal of Heat and Mass Transfer*. 2018;**120**:33-41

[49] Khodadadi JM, Fan L, Babaei H. Thermal conductivity enhancement of nanostructure-based colloidal suspensions utilized as phase change materials for thermal energy storage: A review. *Renewable and Sustainable Energy Reviews*. 2013;**24**:418-444

[50] Khodadadi JM, Hosseinzadeh SF. Nanoparticle-enhanced phase change materials (NEPCM) with great potential for improved thermal energy storage. *International Communications in Heat and Mass Transfer*. 2007;**34**:534-543

[51] Chieruzzi M, Cerritelli GF, Miliozzi A, Kenny JM. Effect of nanoparticles on heat capacity of nanofluids based on molten salts as PCM for thermal energy storage. *Nanoscale Research Letters*. 2013;**8**:448

[52] Kibria MA, Anisur MR, Mahfuz MH, Saidur R, Metselaar IHSC. A review on thermophysical properties of nanoparticle dispersed phase change materials. *Energy Conversion and Management*. 2015;**95**:69-89

[53] Arasu AV, Mujumdar AS. Numerical study on melting of paraffin wax with Al_2O_3 in a square enclosure. *International Communications in Heat and Mass Transfer*. 2012;**39**:8-16

[54] Fan L, Khodadadi JM. An experimental investigation of enhanced thermal conductivity and expedited unidirectional freezing of cyclohexane-based nanoparticle suspensions utilized as nano-enhanced phase change

materials (NePCM). *International Journal of Thermal Sciences*. 2012;**62**:120-126

[55] Sciacovelli A, Colella F, Verda V. Melting of PCM in a thermal energy storage unit: Numerical investigation and effect of nanoparticle enhancement. *International Journal of Energy Research*. 2013;**37**:1610-1623

[56] Dhaidan NS, Khodadadi JM, Al-Hattab TA, Al-Mashat SM. Experimental and numerical investigation of melting of phase change material/nanoparticle suspensions in a square container subjected to a constant heat flux. *International Journal of Heat and Mass Transfer*. 2013;**66**:672-683

[57] Dhaidan NS, Khodadadi JM, Al-Hattab TA, Al-Mashat SM. Experimental and numerical study of constrained melting of n-octadecane with CuO nanoparticle dispersions in a horizontal cylindrical capsule subjected to a constant heat flux. *International Journal of Heat and Mass Transfer*. 2013;**67**:523-534

[58] Zeng Y, Fan L-W, Xiao Y-Q, Yu Z-T, Cen K-F. An experimental investigation of melting of nanoparticle-enhanced phase change materials (NePCMs) in a bottom-heated vertical cylindrical cavity. *International Journal of Heat and Mass Transfer*. 2013;**66**:111-117

[59] Chandrasekaran P, Cheralathan M, Kumaresan V, Velraj R. Enhanced heat transfer characteristics of water based copper oxide nanofluid PCM (phase change material) in a spherical capsule during solidification for energy efficient cool thermal storage system. *Energy*. 2014;**72**:636-642

[60] Altohamy AA, Abd Rabbo MF, Sakr RY, Attia AAA. Effect of water based Al_2O_3 nanoparticle PCM on cool storage performance. *Applied Thermal Engineering*. 2015;**84**:331-338

- [61] Sathishkumar A, Kumaresan V, Velraj R. Solidification characteristics of water based graphene nanofluid PCM in a spherical capsule for cool thermal energy storage applications. *International Journal of Refrigeration*. 2016;**66**:73-83
- [62] Arici M, Tutuncu E, Kan M, Karabay H. Melting of nanoparticle-enhanced paraffin wax in a rectangular enclosure with partially active walls. *International Journal of Heat and Mass Transfer*. 2017;**104**:7-17
- [63] Parsazadeh M, Duan X. Numerical and statistical study on melting of nanoparticle enhanced phase change material in a shell-and-tube thermal energy storage system. *Applied Thermal Engineering*. 2017;**111**: 950-960
- [64] Pahamli Y, Hosseini MJ, Ranjbar AA, Bahrampoury R. Effect of nanoparticle dispersion and inclination angle on melting of PCM in a shell and tube heat exchanger. *Journal of the Taiwan Institute of Chemical Engineers*. 2017;**81**:316-334
- [65] Motahar S, Alemrajabi AA, Khodabandeh R. Experimental study on solidification process of a phase change material containing TiO₂ nanoparticles for thermal energy storage. *Energy Conversion and Management*. 2017;**138**: 162-170
- [66] Elbahjaoui R, El Qarnia H. Transient behavior analysis of the melting of nanoparticle-enhanced phase change material inside a rectangular latent heat storage unit. *Applied Thermal Engineering*. 2017;**112**:720-738
- [67] Wang F, Zhang C, Liu J, Fang X, Zhang Z. Highly stable graphite nanoparticle-dispersed phase change emulsions with little supercooling and high thermal conductivity for cold energy storage. *Applied Energy*. 2017; **188**:97-106
- [68] Sheikholeslami M, Ghasemi A, Li Z, Shafee A, Saleem S. Influence of CuO nanoparticles on heat transfer behavior of PCM in solidification process considering radiative source term. *International Journal of Heat and Mass Transfer*. 2018;**126**:1252-1264
- [69] Sheikholeslami M. Finite element method for PCM solidification in existence of CuO nanoparticles. *Journal of Molecular Liquids*. 2018;**265**:347-355
- [70] Sheikholeslami M. Solidification of NEPCM under the effect of magnetic field in a porous thermal energy storage enclosure using CuO nanoparticles. *Journal of Molecular Liquids*. 2018;**263**: 303-315
- [71] Sheikholeslami M, Ghasemi A. Solidification heat transfer of nanofluid in existence of thermal radiation by means of FEM. *International Journal of Heat and Mass Transfer*. 2018;**123**: 418-431
- [72] Li Z, Sheikholeslami M, Samandari M, Shafee A. Nanofluid unsteady heat transfer in a porous energy storage enclosure in existence of Lorentz forces. *International Journal of Heat and Mass Transfer*. 2018;**127**:914-926
- [73] Sheikholeslami M, Li Z, Shafee A. Lorentz force effect on NEPCM heat transfer during solidification in a porous energy storage system. *International Journal of Heat and Mass Transfer*. 2018;**127**:665-674
- [74] Naghavi MS, Ong KS, Mehrali M, Badruddin IA, Metselaar HSC. A state-of-the-art review on hybrid heat pipe latent heat storage systems. *Energy Conversion and Management*. 2015;**105**: 1178-1204
- [75] Tiari S, Mahdavi M, Qiu S. Experimental study of a latent heat thermal energy storage system assisted by a heat pipe network. *Energy*

- Conversion and Management. 2017;**153**: 362-373
- [76] Robak CW, Bergman TL, Faghri A. Enhancement of latent heat energy storage using embedded heat pipes. *International Journal of Heat and Mass Transfer*. 2011;**54**:3476-3484
- [77] Liu X, Fang G, Chen Z. Dynamic charging characteristics modeling of heat storage device with heat pipe. *Applied Thermal Engineering*. 2011;**31**: 2902-2908
- [78] Xiaohong G, Bin L, Yongxian G, Xiugan Y. Two-dimensional transient study thermal analysis of PCM canister of a heat pipe receiver under microgravity. *Applied Thermal Engineering*. 2011;**31**:735-741
- [79] Nithyanandam K, Pitchumani R. Analysis and optimization of a latent thermal energy storage system with embedded heat pipes. *International Journal of Heat and Mass Transfer*. 2011; **54**:4596-4610
- [80] Sharifi N, Wang S, Bergman TL, Faghri A. Heat pipe-assisted melting of a phase change material. *International Journal of Heat and Mass Transfer*. 2012;**55**:3458-3469
- [81] Shabgard H, Robak CW, Bergman TL, Faghri A. Heat transfer and exergy analysis of cascaded latent heat storage with gravity-assisted heat pipes for concentrating solar power applications. *Solar Energy*. 2012;**86**:816-830
- [82] Nithyanandam K, Pitchumani R. Computational studies on a latent thermal energy storage system with integral heat pipes for concentrating solar power. *Applied Energy*. 2013;**103**: 400-415
- [83] Sharifi N, Bergman TL, Allen MJ, Faghri A. Melting and solidification enhancement using a combined heat pipe, foil approach. *International Journal of Heat and Mass Transfer*. 2014;**78**:930-941
- [84] Jung EG, Boo JH. Thermal analytical model of latent thermal storage with heat pipe heat exchanger for concentrated solar power. *Solar Energy*. 2014;**102**:318-332
- [85] Lorente S, Bejan A, Niu JL. Phase change heat storage in an enclosure with vertical pipe in the center. *International Journal of Heat and Mass Transfer*. 2014;**72**:329-335
- [86] Tiari S, Qiu S, Mahdavi M. Numerical study of finned heat pipe-assisted thermal energy storage system with high temperature phase change material. *Energy Conversion and Management*. 2015;**89**:833-842
- [87] Sharifi N, Faghri A, Bergman TL, Andraka CE. Simulation of heat pipe-assisted latent heat thermal energy storage with simultaneous charging and discharging. *International Journal of Heat and Mass Transfer*. 2015;**80**:170-179
- [88] Liu Z-h, Zheng B-c, Wang Q, Li S-S. Study on the thermal storage performance of a gravity-assisted heat-pipe thermal storage unit with granular high-temperature phase-change materials. *Energy*. 2015;**81**:754-765
- [89] Zhao J, Rao Z, Liu C, Li Y. Experimental investigation on thermal performance of phase change material coupled with closed-loop oscillating heat pipe (PCM/CLOHP) used in thermal management. *Applied Thermal Engineering*. 2016;**93**:90-100
- [90] Tiari S, Qiu S, Mahdavi M. Discharging process of a finned heat pipe-assisted thermal energy storage system with high temperature phase change material. *Energy Conversion and Management*. 2016;**118**:426-437
- [91] Zhao J, Rao Z, Liu C, Li Y. Experiment study of oscillating heat

- pipe and phase change materials coupled for thermal energy storage and thermal management. *International Journal of Heat and Mass Transfer*. 2016;**99**:252-260
- [92] Motahar S, Khodabandeh R. Experimental study on the melting and solidification of a phase change material enhanced by heat pipe. *International Communications in Heat and Mass Transfer*. 2016;**73**:1-6
- [93] Amini A, Miller J, Jouhara H. An investigation into the use of the heat pipe technology in thermal energy storage heat exchangers. *Energy*. 2017;**136**:163-172
- [94] Naghavi MS, Ong KS, Badruddin IA, Mehrali M, Metselaar HSC. Thermal performance of a compact design heat pipe solar collector with latent heat storage in charging/discharging modes. *Energy*. 2017;**127**:101-115
- [95] Pan C, Vermaak N, Romero C, Neti S, Hoenig S, Chen C-H. Efficient optimization of a longitudinal finned heat pipe structure for a latent thermal energy storage system. *Energy Conversion and Management*. 2017;**153**: 93-105
- [96] Zhao J, Qu J, Rao Z. Thermal characteristic and analysis of closed loop oscillation heat pipe/phase change material (CLOHP/PCM) coupling module with different working media. *International Journal of Heat and Mass Transfer*. 2018;**126**:257-266
- [97] Sheikholeslami M. Numerical modeling of nano enhanced PCM solidification in an enclosure with metallic fin. *Journal of Molecular Liquids*. 2018;**259**:424-438
- [98] Rabienataj Darzi AA, Jourabian M, Farhadi M. Melting and solidification of PCM enhanced by radial conductive fins and nanoparticles in cylindrical annulus. *Energy Conversion and Management*. 2016;**118**:253-263
- [99] Lohrasbi S, Sheikholeslami M, Ganji DD. Multi-objective RSM optimization of fin assisted latent heat thermal energy storage system based on solidification process of phase change material in presence of copper nanoparticles. *Applied Thermal Engineering*. 2017;**118**: 430-447
- [100] Parsazadeh M, Duan X. Numerical study on the effects of fins and nanoparticles in a shell and tube phase change thermal energy storage unit. *Applied Energy*. 2018;**216**:142-156
- [101] Hossain R, Mahmud S, Dutta A, Pop I. Energy storage system based on nanoparticle-enhanced phase change material inside porous medium. *International Journal of Thermal Sciences*. 2015;**91**:49-58
- [102] Tasnim SH, Hossain R, Mahmud S, Dutta A. Convection effect on the melting process of nano-PCM inside porous enclosure. *International Journal of Heat and Mass Transfer*. 2015;**85**: 206-220
- [103] Srivatsa PVSS, Baby R, Balaji C. Numerical investigation of PCM based heat sinks with embedded metal foam/ crossed plate fins. *Numerical Heat Transfer, Part A: Applications*. 2014;**66**: 1131-1153
- [104] Mahdi JM, Nsofor EC. Melting enhancement in triplex-tube latent thermal energy storage system using nanoparticles-fins combination. *International Journal of Heat and Mass Transfer*. 2017;**109**:417-427
- [105] Mahdi JM, Nsofor EC. Solidification enhancement of PCM in a triplex-tube thermal energy storage system with nanoparticles and fins. *Applied Energy*. 2018;**211**:975-986

- [106] Mahdi JM, Nsofor EC. Melting enhancement in triplex-tube latent heat energy storage system using nanoparticles-metal foam combination. *Applied Energy*. 2017;**191**:22-34
- [107] Mahdi JM, Nsofor EC. Solidification enhancement in a triplex-tube latent heat thermal energy storage system using nanoparticles-metal foam combination. *Energy*. 2017;**126**:501-512
- [108] Brinkman HC. The viscosity of concentrated suspensions and solutions. *The Journal of Chemical Physics*. 1952; **20**(4):571
- [109] Kakac S, Pramuanjaroenkij A. Review of convective heat transfer enhancement with nanofluids. *International Journal of Heat and Mass Transfer*. 2009;**52**:3187-3196
- [110] Wang M, Wang J, Pan N, Chen S. Mesoscopic predictions of the effective thermal conductivity for microscale random porous media. *Physical Review E*. 2007;**75**:036702
- [111] Ren Q, He Y-L, Su K-Z, Chan CL. Investigation of the effect of metal foam characteristics on the PCM melting performance in a latent heat thermal energy storage unit by pore-scale lattice Boltzmann modeling. *Numerical Heat Transfer, Part A: Applications*. 2017;**72**: 745-764
- [112] Chen S, Doolen GD. Lattice Boltzmann method for fluid flows. *Annual Review of Fluid Mechanics*. 1998;**30**:329-364
- [113] Chen L, Kang Q, Mu Y, He Y-L, Tao W-Q. A critical review of the pseudopotential multiphase lattice Boltzmann model: Methods and applications. *International Journal of Heat and Mass Transfer*. 2014;**76**: 210-236
- [114] Li Q, Luo KH, Kang QJ, He YL, Chen Q, Liu Q. Lattice Boltzmann methods for multiphase flow and phase-change heat transfer. *Progress in Energy and Combustion Science*. 2016;**52**: 62-105
- [115] Zhang J. Lattice Boltzmann method for microfluidics: Models and applications. *Microfluidics and Nanofluidics*. 2010;**10**:1-28
- [116] Miller W. The lattice Boltzmann method: A new tool for numerical simulation of the interaction of growth kinetics and melt flow. *Journal of Crystal Growth*. 2001;**230**(1-2):263-269
- [117] Rasin I, Miller W, Succi S. Phase-field lattice kinetic scheme for the numerical simulation of dendritic growth. *Physical Review E*. 2005;**72**: 066705
- [118] Huang RZ, Wu HY. An immersed boundary-thermal lattice Boltzmann method for solid-liquid phase change. *Journal of Computational Physics*. 2014; **277**:305-319
- [119] Jiaung WS, Ho JR, Kuo CP. Lattice Boltzmann method for the heat conduction problem with phase change. *Numerical Heat Transfer, Part B: Fundamentals*. 2001;**39**:167-187
- [120] Huber C, Parmigiani A, Chopard B, Manga M, Bachmann O. Lattice Boltzmann model for melting with natural convection. *International Journal of Heat and Fluid Flow*. 2008; **29**(5):1469-1480
- [121] Eshraghi M, Felicelli SD. An implicit lattice Boltzmann model for heat conduction with phase change. *International Journal of Heat and Mass Transfer*. 2012;**55**(9-10):2420-2428
- [122] Feng Y, Li H, Li L, Lin B, Wang T. Numerical investigation on the melting of nanoparticle-enhanced phase change (NEPCM) in a bottom-heated rectangular cavity using lattice Boltzmann method. *International*

- Journal of Heat and Mass Transfer. 2015; **81**:415-425
- [123] Huang RZ, Wu HY, Cheng P. A new lattice Boltzmann model for solid-liquid phase change. International Journal of Heat and Mass Transfer. 2013;**59**:295-301
- [124] Huang RZ, Wu HY. Phase interface effects in the total enthalpy-based lattice Boltzmann model for solid-liquid phase change. Journal of Computational Physics. 2015;**294**:346-362
- [125] Li D, Ren Q, Tong Z-X, He Y-L. Lattice Boltzmann models for axisymmetric solid-liquid phase change. International Journal of Heat and Mass Transfer. 2017;**112**:795-804
- [126] Li D, Tong Z-X, Ren Q, He Y-L, Tao W-Q. Three-dimensional lattice Boltzmann models for solid-liquid phase change. International Journal of Heat and Mass Transfer. 2017;**115**:1334-1347
- [127] Su Y, Davidson JH. A new mesoscopic scale timestep adjustable non-dimensional lattice Boltzmann method for melting and solidification heat transfer. International Journal of Heat and Mass Transfer. 2016;**92**: 1106-1119
- [128] Wu W, Zhang S, Wang S. A novel lattice Boltzmann model for the solid-liquid phase change with the convection heat transfer in the porous media. International Journal of Heat and Mass Transfer. 2017;**104**:675-687
- [129] Gao D, Tian F-B, Chen Z, Zhang D. An improved lattice Boltzmann method for solid-liquid phase change in porous media under local thermal non-equilibrium conditions. International Journal of Heat and Mass Transfer. 2017; **110**:58-62
- [130] Liu Q, He Y-L, Li Q. Enthalpy-based multiple-relaxation-time lattice Boltzmann method for solid-liquid phase-change heat transfer in metal foams. Physical Review E. 2017;**96**:023303
- [131] Yu Z, Fan LS. Multirelaxation-time interaction-potential-based lattice Boltzmann model for two phase flow. Physical Review E. 2010;**82**:046708
- [132] Li Q, Luo KH, Li XJ. Lattice Boltzmann modeling of multiphase flows at large density ratio with an improved pseudopotential model. Physical Review E. 2013;**87**:053301
- [133] Hu A, Li L, Uddin R. Force method in a pseudo-potential lattice Boltzmann model. Journal of Computational Physics. 2015;**294**:78-89
- [134] Huang R, Wu H. Third-order analysis of pseudopotential lattice Boltzmann model for multiphase flow. Journal of Computational Physics. 2016; **327**:121-139
- [135] McCracken ME, Abraham J. Multiple-relaxation-time lattice-Boltzmann model for multiphase flow. Physical Review E. 2005;**71**:036701
- [136] Guo Z, Zheng C. Analysis of lattice Boltzmann equation for microscale gas flows: Relaxation times, boundary conditions and the Knudsen layer. International Journal of Fluid Dynamics. 2008;**22**:465-473
- [137] Lallemand P, Luo LS. Theory of the lattice Boltzmann method: Dispersion, dissipation, isotropy, Galilean invariance, and stability. Physical Review E. 2000;**61**:6546-6562
- [138] Huang R, Wu H. Total enthalpy-based lattice Boltzmann method with adaptive mesh refinement for solid-liquid phase change. Journal of Computational Physics. 2016;**315**:65-83
- [139] Zhao-Li G, Chu-Guang Z, Bao-Chang S. Non-equilibrium extrapolation method for velocity and pressure boundary conditions in the lattice

- Boltzmann method. Chinese Physics. 2002;**11**(4):366-374
- [140] Guo Z, Zheng C. An extrapolation method for boundary conditions in lattice Boltzmann method. Physics of Fluids. 2002;**14**(6):2007-2010
- [141] Yoshida H, Kobayashi T, Hayashi H, Kinjo T, Washizu H, Fukuzawa K. Boundary condition at a two-phase interface in the lattice Boltzmann method for the convection-diffusion equation. Physical Review E. 2014;**90**:013303
- [142] Ren Q, Chan CL. GPU accelerated numerical study of PCM melting process in an enclosure with internal fins using lattice Boltzmann method. International Journal of Heat and Mass Transfer. 2016;**100**:522-535
- [143] Hu H, Argyropoulos SA. Mathematical modeling of solidification and melting: A review. Modelling and Simulation in Materials Science and Engineering. 1996;**4**:371-396
- [144] Mencinger J. Numerical simulation of melting in two-dimensional cavity using adaptive grid. Journal of Computational Physics. 2004;**198**(1): 243-264
- [145] Jany P, Bejan A. Scaling theory of melting with natural convection in an enclosure. International Journal of Heat and Mass Transfer. 1988;**31**:1221-1235
- [146] CUDA Toolkit Documentation V9.2, NVIDIA CORPORATION: <https://docs.nvidia.com/cuda/>
- [147] Zhao Y. Lattice Boltzmann based PDE solver on the GPU. The Visual Computer. 2008;**24**:323-333
- [148] Riegel E, Indinger T, Adams NA. Implementation of a Lattice-Boltzmann method for numerical fluid mechanics using the NVIDIA CUDA technology. Computer Science—Research and Development. 2009;**23**:241-247
- [149] Obrecht C, Kuznik F, Tourancheau B, Roux J-J. A new approach to the lattice Boltzmann method for graphics processing units. Computers & Mathematics with Applications. 2011;**61**: 3628-3638
- [150] Obrecht C, Kuznik F, Tourancheau B, Roux J-J. Multi-GPU implementation of the lattice Boltzmann method. Computers & Mathematics with Applications. 2013;**65**:252-261
- [151] Habich J, Feichtinger C, Kostler H, Hager G, Wellein G. Performance engineering for the lattice Boltzmann method on GPGPUS: Architectural requirements and performance results. Computers & Fluids. 2013;**80**:276-282
- [152] Ren Q, Chan CL. Natural convection with an array of solid obstacles in an enclosure by lattice Boltzmann method on a CUDA computation platform. International Journal of Heat and Mass Transfer. 2016;**93**:273-285
- [153] Ren Q, Chan CL. Numerical study of double-diffusive convection in a vertical cavity with Soret and Dufour effects by lattice Boltzmann method on GPU. International Journal of Heat and Mass Transfer. 2016;**93**:538-553
- [154] Ren Q, Chan CL. Numerical simulation of a 2D electrothermal pump by lattice Boltzmann method on GPU. Numerical Heat Transfer, Part A: Applications. 2016;**69**:677-693
- [155] Ren Q. Investigation of pumping mechanism for non-Newtonian blood flow with AC electrothermal forces in a microchannel by hybrid boundary element method and immersed boundary-lattice Boltzmann method. Electrophoresis. 2018;**39**:1329-1338
- [156] Jourabian M, Farhadi M, Sedighi K, Darzi AAR, Vazifeshenas Y. International Journal for Numerical Methods in Fluids. 2012;**70**:313-325

- [157] Talati F, Taghilou M. Lattice Boltzmann application on the PCM solidification within a rectangular finned container. *Applied Thermal Engineering*. 2015;**83**:108-120
- [158] Jourabian M, Farhadi M, Rabienataj Darzi AA. Outward melting of ice enhanced by Cu nanoparticles inside cylindrical horizontal annulus: Lattice Boltzmann approach. *Applied Mathematical Modelling*. 2013;**37**: 8813-8825
- [159] Jourabian M, Farhadi M, Sedighi K. On the expedited melting of phase change material (PCM) through dispersion of nanoparticles in the thermal storage unit. *Computers and Mathematics with Applications*. 2014; **67**:1358-1372
- [160] Tao YB, You Y, He YL. Lattice Boltzmann simulation on phase change heat transfer in metal foams/paraffin composite phase change material. *Applied Thermal Engineering*. 2016;**93**: 476-485
- [161] Li X, Ma T, Liu J, Zhang H, Wang Q. Pore-scale investigation of gravity effects on phase change heat transfer characteristics using lattice Boltzmann method. *Applied Energy*. 2018;**222**: 92-103
- [162] Luo K, Yao F-J, Yi H-L, Tan H-P. Lattice Boltzmann simulation of convection melting in complex heat storage systems filled with phase change materials. *Applied Thermal Engineering*. 2015;**86**:238-250
- [163] Huo Y, Rao Z. Lattice Boltzmann investigation on phase change of nanoparticle-enhanced phase change material in a cavity with separate plate. *Energy Conversion and Management*. 2017;**154**:420-429
- [164] Gao D, Chen Z, Zhang D, Chen L. Lattice Boltzmann modeling of melting of phase change materials in porous media with conducting fins. *Applied Thermal Engineering*. 2017;**118**:315-327
- [165] Jourabian M, Farhadi M, Rabienataj Darzi AA. Constrained ice melting around one cylinder in horizontal cavity accelerated using three heat transfer enhancement techniques. *International Journal of Thermal Sciences*. 2018;**125**: 231-247
- [166] Ren Q, Meng F, Guo P. A comparative study of PCM melting process in a heat pipe-assisted LHTES unit enhanced with nanoparticles and metal foams by immersed boundary-lattice Boltzmann method at pore-scale. *International Journal of Heat and Mass Transfer*. 2018;**121**:1214-1228